

# Discovery of 17 new sharp-lined Ap stars with magnetically resolved lines<sup>\*</sup>

L. M. Freyhammer<sup>1†</sup>, V. G. Elkin<sup>1</sup>, D. W. Kurtz<sup>1</sup>, G. Mathys<sup>2</sup> and P. Martinez<sup>3</sup>

<sup>1</sup>Centre for Astrophysics, University of Central Lancashire, Preston PR1 2HE

<sup>2</sup>European Southern Observatory, Casilla 19001, Santiago 19, Chile

<sup>3</sup>South African Astronomical Observatory (SAAO), PO Box 9, Observatory 7935, South Africa

Draft 4 December 2018; Accepted . Received ; in original form

## ABSTRACT

Chemically peculiar A stars (Ap) are extreme examples of the interaction of atomic element diffusion processes with magnetic fields in stellar atmospheres. The rapidly oscillating Ap stars provide a means for studying these processes in 3D and are at the same time important for studying the pulsation excitation mechanism in A stars. As part of the first comprehensive, uniform, high resolution spectroscopic survey of Ap stars, which we are conducting in the southern hemisphere with the Michigan Spectral Catalogues as the basis of target selection, we report here the discovery of 17 new magnetic Ap stars having spectroscopically resolved Zeeman components from which we derive magnetic field moduli in the range 3 – 30 kG. Among these are 1) the current second-strongest known magnetic A star, 2) a double-lined Ap binary with a magnetic component and 3) an A star with particularly peculiar and variable abundances. Polarimetry of these stars is needed to constrain their field geometries and to determine their rotation periods. We have also obtained an additional measurement of the magnetic field of the Ap star HD 92499.

**Key words:** stars: – stars: binaries: spectroscopic – stars: chemically peculiar – stars: magnetic fields – stars: variables: other

## 1 INTRODUCTION

The study of chemically peculiar A stars with magnetic fields has ramifications for several other branches of astrophysics. The interaction among strong magnetic fields, atomic diffusion and energy transfer in (or above) the upper atmospheres of non-degenerate stars has direct implications for observed stellar abundances and for the instability of stellar pulsations in  $\beta$  Cephei and sdB stars. The magnetic field lines guide the diffusing elements, so that some ions will be concentrated where the field lines are vertical while others will group where the lines are horizontal (e.g. Michaud, Charland & Megessier 1981). The very different magnetic field strengths, orientations and geometries, as well as the great variety of abundance distributions for Ap stars are therefore particularly informative.

Magnetic fields affect spectroscopic lines through, e.g., broadening, intensification and Zeeman splitting of the in-

trinsic lines (Mathys 1989). Several cool Ap stars show light and spectral variability that follow the stellar rotation, and such stars are known as  $\alpha^2$  Canum Venaticorum ( $\alpha^2$  CVn) variables. Wolff & Wolff (1971) demonstrated that the observed light, spectrum and magnetic variations are related. In particular, they suggested that photometric variability may result from a redistribution of flux either by variations in line blanketing or opacity, such as enhanced absorption at rare earth maximum. The light variability may vary with that of the rare earths which appear to be concentrated predominantly near the region of the strongest magnetic field or that of the negative pole. Thus can light variability be linked to magnetic field variability which, for oblique rotators, follows the stellar rotation.

Magnetic activity cycles similar to the solar 11-y cycle are observed in F–M stars (Baliunas et al. 1995) and are related to chromospheric activity. However, chromospheres have not been unambiguously detected in Ap stars. Finally, magnetic fields drive winds through Alfvén waves or other magneto-hydrodynamic waves (Linsky 1999).

The chemically peculiar B, A and F stars (henceforth Ap stars) have globally organised, typically dipole or

<sup>\*</sup> Based on observations collected at the European Southern Observatory, Paranal, Chile, as part of programmes 078.D-0080(A), 078.D-0192(A), 072.D-0138(A).

<sup>†</sup> E-mail: lmfreyhammer@uclan.ac.uk

quadrupole fields that with an axis obliquely inclined to the rotation axis of the star so that, for dipolar fields, one or both magnetic poles come into, or out of, view with rotation. The full geometry of the field may hence be visible for stars with favourably oriented rotation and magnetic axes, which in turn makes it possible to use the Zeeman Doppler imaging technique to create magnetic field maps. Among the Ap stars is Babcock's star = HD 215441 (Babcock 1960), the non-degenerate star with the strongest field known, 34.4 kG. The only other published cases with extremely strong fields are: HD 137509,  $\langle B \rangle = 29$  kG (Kochukhov 2006), HD 154708,  $\langle B \rangle = 24.5$  kG (Hubrig et al. 2005) and HD 178892,  $\langle B \rangle = 18.0$  kG (Ryabchikova et al. 2006a).

The atmospheres of Ap stars are complex to interpret. As a consequence of vertical abundance stratification, and non-standard temperature gradients, even theoretical modelling of hydrogen line profiles, such as the core-wing anomaly in the H $\alpha$  lines (Cowley et al. 2001), is not yet completely successful (Kochukhov, Bagnulo & Barklem 2002). However, the observational and theoretical efforts in understanding the Ap atmospheric processes may eventually prove 'worth the candle' thanks to their general applicability; the Ap stars are the most extreme examples of magnetic fields and atomic diffusion in non-degenerate stars, processes common in most other stars. Examples of studies of atmospheric abundance stratification in a cool Ap star subgroup, the rapidly oscillating Ap (roAp) stars are given by Wade et al. (2001); Ryabchikova et al. (2002); Ryabchikova, Leone & Kochukhov (2005). These studies are in agreement with each other, in general: Fe is concentrated by gravitational settling in the observable layer between  $-1 < \log \tau_{5000} < 0$  and Pr and Nd are concentrated by radiative levitation above  $\log \tau_{5000} = -5$ . The Pr and Nd forming layers are above the line forming layer of the narrow core of the H $\alpha$  line which in standard A star models is in the range  $-4 < \log \tau_{5000} < -2$ .

Magnetic field measurements are mostly based on difficult, indirect measurements, such as magnetic broadening of spectral lines and spectropolarimetric observations of longitudinal magnetic fields or the line-of-sight field component. The mean longitudinal magnetic field (or, the longitudinal field)  $\langle B_z \rangle$  is a weighted average over the visible stellar disk of the component of the magnetic vector along the line of sight (Mathys 1989), and is typically at least 3 times weaker than the mean magnetic field modulus  $\langle B \rangle$  (see Sect. 3.2.3 for definition of this). The first large survey for magnetic fields in non-degenerate stars was done by Babcock (1958). It has since been followed by many other studies of individual stars or groups of stars (e.g., Borra and Landstreet 1979; Bohlender et al. 1993). Recent searches for magnetic stars were carried out by Kudryavtsev et al. (2006) who discovered  $\sim 70$  magnetic stars, and by Hubrig et al. (2006) who discovered 57 magnetic Ap stars. The total number of firmly established magnetic chemically peculiar main-sequence stars is currently  $\sim 350$  (Romanyuk, 2008, in prep.) For a significant fraction of these magnetic stars the variation in the longitudinal magnetic field has been measured as a function of rotation period (see, e.g., Mathys 1991).

Such curves provide valuable information about the global geometrical structure of magnetic fields. Better and more reliable measurements are necessary to obtain a complete understanding of the many phenomena related to mag-

netic fields. For this purpose, magnetic Ap stars with resolved magnetically split lines provide extremely favourable conditions, since one can determine in a straightforward, mostly approximation-free, model-independent manner, and with particularly good precision, the mean magnetic field modulus (Mathys et al. 1997). However, in spite of many studies (e.g., Mathys et al. 1997; Hubrig & Nesvacil 2007), only 51 such stars were known (Hubrig & Nesvacil 2007), prior to this work. Our discovery of 17 new such stars therefore significantly increases the number known.

At present, 40 roAp stars are known (see, e.g., Kurtz et al. 2006b; González et al. 2008), although several surveys have searched for rapid pulsation in Ap stars, such as Nelson & Kreidl (1993); Martinez & Kurtz (1994); Handler & Paunzen (1999); Ashoka et al. (2000); Weiss et al. (2000); Dorokhova & Dorokhov (2005). For a (non-exhaustive) list of spectroscopic studies of roAp stars, see Kurtz et al. (2006a). The roAp stars are thought to be characterised by, e.g., the H $\alpha$  *core-wing anomaly* and by an *ionization disequilibrium* for Nd II and Nd III and for Pr II and Pr III (Ryabchikova et al. 2004), the latter caused by stratification of those two elements to levels above  $\log \tau_{5000} \sim -5$  by atomic diffusion. Other typical spectral characteristics are strong magnetic fields, wing-nib anomaly in Ca II K (Cowley, Hubrig & Kamp 2006), and strong abundances of rare earth elements and relatively slow rotation. It is therefore possible to identify promising roAp star candidates with a single, high signal-to-noise ratio, high-resolution spectrum before spending time on a large telescope with fast spectroscopy to search for rapid pulsations.

In 2006 we therefore began a systematic survey of cool Ap stars in the photometric 'Cape cool Ap star catalogue' (Martinez 1993) to identify roAp candidates based generally on a single high-resolution spectrum of each star. The Cape catalogue gives Strömgren *wvby* and  $\beta$  photometry for over 500 (almost all) of the SrCrEu subclass of cool Ap stars listed in the Michigan spectral catalogues, volumes 1 – 4 (Houk 1978, 1982; Houk & Cowley 1975; Houk & Smith-Moore 1988). Perhaps surprisingly – given the importance of the Ap stars to stellar astrophysics, and the long history of their study – there is no large-scale, uniform spectroscopic survey such as the one we are now conducting. We expect the data set to be a rich source of discoveries, and to be the basis of uniform statistical analyses of many of the astrophysically interesting characteristics of the class.

Our first observing season is finished and of 140 stars, we identified dozens of stars with magnetically intensified, broadened or even resolved lines. Of these, 17 are new detections with magnetically resolved or partially resolved lines, in particular for the Zeeman doublet Fe II 6149.258 Å (Figs 1–2). As pointed out by Mathys et al. (1997), this line is particularly important as a diagnostic for a magnetic field as the splitting provides a direct measure of the mean magnetic field, and furthermore because iron is usually rather homogeneously distributed over the surface of Ap stars.

This is the discovery paper for the new Ap stars with magnetically resolved lines, and we provide magnetic field strengths, projected rotation velocities and selected relative abundance estimates. Of particular interest, we discovered a new star with an extremely large magnetic field; a highly peculiar magnetic star; and an uncommon magnetic

**Table 1.** Observing log indicating target, equatorial coordinates, instrument (UVES, ‘U’ or FEROS, ‘F’), mid-exposure heliocentric Julian Date (HJD), exposure time, number of co-added spectra, if any, and  $S/N$ . The  $S/N$  ratio were measured in the 2-D spectra around 5500 Å. For co-added spectra, HJD gives the mid-series time, and the total exposure time and combined  $S/N$  are given.

Star HD	$\alpha_{2000.0}$ (h:m:s)	$\delta_{2000.0}$ (°:':")	Ins.	HJD (−2450000)	$t_{\text{exp}}$ (s)	$n$	$S/N$
33629	05:10:05.8	−33:46:46	F	4138.56813	800		198
42075	06:07:36.9	−26:37:16	F	4138.62481	800		195
			F	4141.57144	800		247
			U	4172.50223	450		273
44226	06:19:34.8	−25:19:42	F	4138.65922	1100		170
46665	06:33:41.1	−22:41:45	F	4138.69450	1200		170
			U	4173.48552	460	2	185
47009	06:35:48.6	−13:44:50	F	4138.70824	800		159
52847	07:01:46.3	−23:06:20	F	4138.72195	300		165
			U	4173.50404	300		311
55540	07:12:30.4	−21:03:54	F	4138.75030	1100		165
			F	4139.68374	1200		223
			F	4141.55994	1100		231
			U	4173.49684	350		177
69013	08:14:29.0	−15:46:32	F	4140.60574	900		153
72316	08:30:58.5	−33:38:04	F	4140.62692	500		171
75049	08:45:33.1	−50:43:58	F	4141.66711	1500	2	265
			U	4171.50465	900	4	285
88701	10:13:00.2	−37:30:12	F	4140.69708	720		157
92499	10:40:08.6	−43:04:50	F	4138.80452	600		178
			F	4139.66861	900		223
			F	4141.73381	900		238
			U	4172.49146	630	4	281
96237	11:05:34.0	−25:01:09	F	4138.82842	1100		195
			U	4173.51530	300		152
110274	12:41:31.0	−58:55:24	F	4138.88351	900		169
			F	4141.82828	900		192
			U	4172.90849	500		212
117290	13:30:13.2	−49:07:59	F	4139.76263	900		190
			F	4141.86589	900		221
			U	4171.92209	600	2	233
121661	13:58:42.4	−62:43:07	F	4141.78480	350		156
			U	4171.91084	600	2	311
135728AB	15:17:38.8	−31:27:32	F	4139.86100	500		188
			U	4172.92442	300		257
143487	16:01:44.2	−30:54:57	F	4140.82232	900		153
			U	4173.91731	960	12	308

Ap star in a relatively close binary system. We also re-observed the recently discovered magnetic Ap star HD 92499 (Hubrig & Nesvacil 2007) to check for stability of its magnetic field strength, abundances and radial velocity.

In the following sections, we describe the selection and observation of the targets along with the data reduction in Sect. 2. Then follows the data analyses, including estimation of physical parameters and the magnetic measurements in Sect. 3. Finally we discuss the results in Sect. 4.

## 2 OBSERVATIONS AND DATA REDUCTION

The observations were collected using the Fibre-fed Extended Range Optical Spectrograph (FEROS) with the 2.2-m telescope at La Silla during four nights starting 2007

February 06. Follow-up observations were made for selected stars about one month later with the VLT UV-Visual Echelle Spectrograph (UVES) during three nights starting 2007 March 11 (see the logbook of observations in Table 1). Both instruments are echelle spectrographs and cover the wavelength ranges 3530–9220 Å at the spectral resolution  $R = \lambda/\Delta\lambda = 48000$  (FEROS) and 4970–7010 Å (with a 60-Å wide gap near 6000 Å) at  $R = 110000$  (UVES). The UVES instrument was used with an image slicer and an 0.3 arcsec slit, while FEROS was used with a stellar fibre (1.8 arcsec aperture) while the second (sky) fibre was not used.

The spectra were reduced to 1-D with the respective pipelines provided by ESO with the standard calibration data (bias, flatfield and Thorium-Argon wavelength reference spectra). As indicated in the observing log (Table 1) spectra of the same star were co-added if barycentric velocity corrections were small compared to the bin sizes of the spectra (that was typically the case within 40 min). Table 1 gives the signal-to-noise ratio ( $S/N$  henceforth) of the spectra measured in the 2-D spectra around 5500 Å (for co-added 1-D spectra, the stated  $S/N$  is for the composites). The spectra were normalized to unity continuum level in an iterative manner: major slopes were eliminated with a spline fit to a stacked spectrum of stars with relatively many continuum windows, then a second but more detailed spline fit was made and applied to the spectra on a star-by-star basis. Finally, a detailed spline fit was made by identifying continuum regions through comparison with a synthetic spectrum. This process eliminated flux undulations of lengths similar to the individual echelle orders, but also broad depressions from the strongest diffuse interstellar bands and possibly some of the broadest depressions typical of cool Ap stars.

## 3 DATA ANALYSIS AND RESULTS

### 3.1 Light variability

The photometric databases ASAS (All Sky Automatic Survey, Pojmanski 2002) and the *Hipparcos* catalogue (ESA 1997) were used to search the 18 targets for long-period (days to years) photometric variability. The ASAS light curves are sparsely sampled, typically one measurement per 1–3 nights (causing obvious  $1 \text{ cd}^{-1}$  aliases;  $\text{cd}^{-1}$  is cycles per day), but cover 3–5 years with 300–500 measurements and are therefore well suited to check for variability linked with stellar rotation. Of 5 available apertures we used the largest and for the *V*-band. In seven cases (see notes in Table 2), periodic variability was found above 4–5 mmag amplitude and interpreted as  $\alpha^2 \text{ CVn}$  rotational variability. All frequency searches were made using PERIOD04 (Lenz & Breger 2005) up to the pseudo-Nyquist frequency ( $\sim 0.5 \text{ cd}^{-1}$  for the ASAS data). The shortest period found in these cases is a good candidate for the rotation period for stars where only a single spotted region is within view. However, if two such spots come into view during a rotation cycle (such as orientations where both magnetic poles can be seen during each rotation cycle), then the light curve becomes a double-wave (see Fig. 5) which for similar spots may be mistaken for a single sine wave, thus resulting in a mis-identification of only half the true rotation period.

**Table 2.** Main properties of the 18 magnetic Ap stars. The columns give: (2–6) Strömgren and  $\beta$  indices from Martinez (1993); (7) the revised *Hipparcos* parallax  $\pi$  (van Leeuwen 2007); (8) luminosity based on absolute visual magnitude from Gomez et al. (1998) (except for HD 88701 that was derived directly, assuming no reddening), bolometric corrections based on the relation by Landstreet et al. (2007), and  $M_{\text{bol},\odot} = 4.72$ . (9) Temperature derived from the  $\beta$  index with the  $c_0, \beta$  grid by Moon & Dworetzky (1985);  $\sigma(T_{\text{eff}}) = 200$  K, estimated error. (10) Projected rotation velocity  $v \sin i$ ;  $\sigma(v \sin i) = 1 \text{ km s}^{-1}$ , estimated error, based on line-width measurements and synthetic, rotationally broadened line profiles compared to magnetically insensitive iron lines. (11) Mean magnetic field modulus from direct measurements of the  $\lambda 6149 \text{ \AA}$  line, given as average for all available spectra. For HD 96237, other lines were used instead (see Sect. 3.3.13). Error estimates are based on repeated measurements on different spectra (see Sect. 3.3 for more explanation). (12) Notes on individual stars.  $\alpha^2\text{CVn}$  indicates  $\alpha^2$  Canum Venaticorum variables, based on ASAS photometry, with minimum period indicated in parentheses. Photometric indices and parallax for the double-lined spectroscopic binary (‘SB2’) HD 135728 are for the combined system.

Star HD	$V$ mag	$b - y$ mag	$m_1$ mag	$c_1$ mag	$\beta$ mag	$\pi$ (mas)	$\log L$ $L_{\odot}$	$T_{\text{eff}}$ K	$v \sin i$ $\text{km s}^{-1}$	$\langle B \rangle$ kG	Notes
33629	9.064	0.200	0.231	0.683	2.784			7570	4	$4.76 \pm 0.20$	
42075	8.968	0.205	0.260	0.665	2.788			7590	1	$8.54 \pm 0.02$	
44226	9.492	0.161	0.259	0.771	2.842			8060	2	$4.99 \pm 0.15$	
46665	9.441	0.039	0.255	0.702	2.840	$2.11 \pm 1.16$	$1.50 \pm 0.24$	8050	1	$4.63 \pm 0.13$	
47009	9.070	0.091	0.201	0.885	2.873	$2.75 \pm 1.25$	$1.74 \pm 0.31$	8280	6	$7.36 \pm 0.15$	
52847	8.157	0.101	0.334	0.633	2.843			8060	1	$4.44 \pm 0.01$	
55540	9.498	0.026	0.258	0.774	2.868			8230	5	$12.73 \pm 0.30$	$\alpha^2\text{CVn?}$ (Hensberge et al. 1984), RV variable.
69013	9.456	0.296	0.330	0.400	2.772			7470	4	$4.80 \pm 0.10$	
72316	8.804	-0.001	0.248	0.836	2.840	$2.47 \pm 0.93$	$1.74 \pm 0.27$	8050	6	$5.18 \pm 0.40$	
75049	9.090	-0.054	0.249	0.914	2.906			9700	8	$30.29 \pm 0.08$	$\alpha^2\text{CVn}$ (5.28 yr and 4.05 d)
88701	9.258	0.002	0.225	0.830	2.846	$2.35 \pm 0.99$	$1.41 \pm 0.85$	8080	7	$4.38 \pm 0.35$	$\alpha^2\text{CVn}$ (25.765 d)
92499	8.890	0.179	0.301	0.615	2.812	$3.54 \pm 0.83$	$1.25 \pm 0.20$	7810	2	$8.20 \pm 0.13$	Magnetic <sup>a</sup> . $\alpha^2\text{CVn}$ (> 5 yr)
96237 <sub><math>\phi_1</math></sub>	9.434	0.233	0.261	0.704	2.824	$1.53 \pm 1.15$	$1.61 \pm 0.29$	7930	5	2–3	$\alpha^2\text{CVn}$ (20.9 d)
96237 <sub><math>\phi_2</math></sub>								7800		$2.87 \pm 0.30$	Rapidly changing, highly peculiar.
110274	9.328	0.195	0.208	0.805	2.853	$0.61 \pm 1.30$	$1.82 \pm 0.25$	8130	1	$4.02 \pm 0.38$	$\alpha^2\text{CVn}$ (265.3 d)
117290	9.281	0.152	0.229	0.879	2.867			8230	2	$6.38 \pm 0.02$	$\alpha^2\text{CVn}$ (> 5.7 yr)
121661	8.556	0.036	0.234	0.805	2.866			8230	1	$6.16 \pm 1.14$	$\alpha^2\text{CVn}$ (47.0 d). Magnetic <sup>b</sup> .
135728A	8.602	0.236	0.203	0.931	2.843	$4.27 \pm 1.17$	$1.58 \pm 0.25$	8060	10	0–2.5	SB2 binary.
135728B									2	$3.63 \pm 0.30$	
143487	9.420	0.386	0.262	0.393	2.706			6930	2	$4.23 \pm 0.07$	

Measurements in literature: a)  $\langle B \rangle = 8.5 \pm 0.2 \text{ kG}$  (Hubrig & Nesvacil 2007), b)  $\langle B_s \rangle = 2 \text{ kG}$  and  $\log g = 4.6$  (North & Cramer 1997)

### 3.2 Line analysis

For the purpose of spectral line identification, a synthetic comparison spectrum was produced with SYNTH (Piskunov 1992) using a Kurucz stellar atmosphere model. Atomic line data were taken from the Vienna Atomic Line Database (VALD, Kupka et al. 1999) for ions with increased abundances, mainly for Nd, Pr, Sr, Cr and Eu. Other sources used for line data were the atomic database NIST<sup>1</sup> and the Database on Rare Earth Elements at Mons University (DREAM<sup>2</sup>; Biémont, Palmeri & Quinet 1999) through its implementation in the VALD.

#### 3.2.1 Temperatures and rotational velocities

The spectra of Ap stars have flux distributions that are deformed by strong overabundances of some elements. Calibrations based on Strömgren indices may therefore not provide reliable estimates of temperatures and surface gravity  $\log g$ . The  $\beta$  index, however, remains largely unaffected by this, except in extreme cases – HD 101065, ‘Przybylski’s star’, being the most notorious example. Effective temperatures were thus estimated with the  $c_0, \beta$  grids of Moon & Dworetzky

(1985) using  $\beta$  from Table 2 (from Martinez 1993). We did not use the value of  $c_0$  in these grids, since  $c_0$  is not a reliable indicator of luminosity in Ap stars because of the strong line blanketing in the Strömgren  $v$  band; in any case, temperature in the relevant range is relatively insensitive to  $c_0$ . We fixed  $\beta$  and assumed  $4.0 \leq \log g \leq 4.5$ . The resulting photometric temperatures are given in Table 2. These estimates depend on the actual evolutionary stage and contamination of the spectra by peculiar abundances, and stratification. The relative strengths of the hydrogen lines H8, H $\epsilon$  and of Ca II K are also temperature sensitive and indicate, for ‘normal’ main-sequence stars, temperatures that are 500–1000 K higher for HD 52847, HD 55540, HD 121661 HD 143487, and 500–1000 K lower for HD 42075, HD 44226, HD 92499, HD 117290 and HD 135728AB.

A few of the stars in Table 2 have revised *Hipparcos* parallaxes (van Leeuwen 2007) with relative trigonometric errors of  $\sigma(\pi)/\pi = 0.23\text{--}0.75$  (2.13 for HD 110274). Seven of these have distances and absolute magnitudes,  $M_V$ , given by Gomez et al. (1998), while  $M_V$  for HD 88701 was calculated directly from the parallax assuming no reddening. Gomez et al. (1998) used the statistical LM method (Luri et al. 1996), which is a maximum likelihood method that exploits a combination of proper motion and radial velocity data and trigonometric parallaxes to obtain luminosity calibrations and improved distance estimates. Combined

<sup>1</sup> <http://physics.nist.gov>

<sup>2</sup> <http://w3.umh.ac.be/~astro/dream.shtml>



with our photometric temperatures, these stars form a concentrated group in the ranges  $7810 \leq T_{\text{eff}} \leq 8280$  K and  $0.1 \leq M_V \leq 1.5$ , or  $1.25 \leq \log L/L_{\odot} \leq 1.82$  for bolometric corrections from the relation by Landstreet et al. (2007) and using  $M_{\text{bol},\odot} = 4.72$ . Luminosity errors in Table 2 were estimated from distance errors provided by Gomez et al. (1998), 0.1 mag error in the relation for bolometric correction, and temperature errors (through their influence on the calculated bolometric corrections). Because of the small temperature range, the bolometric corrections are near zero and introduce errors of  $\sim 0.1$  in  $\log L/L_{\odot}$ . Landstreet et al. (2007) derived new bolometric corrections for Ap stars as a function of temperature, using temperatures based on photometric indices. They adopted uniform ‘somewhat optimistic’ uncertainties of about 500 K. Photometric temperature estimates are particularly problematic for Ap stars due to their sensitivity to the large blanketing effects caused by strong absorption in (mostly) rare earth element lines. We find, however, a very good agreement between the predicted and measured bolometric correction for the roAp star  $\alpha$  Cir (Bruntt et al. 2008) with  $T_{\text{eff}}=7420$  K.

Keeping the considerable luminosity errors in mind, and that HD 135728 is a binary, this suggests these are late main-sequence stars around the main-sequence turn-off. Only a single luminous roAp star is known (see Elkin et al. 2005 about the luminous roAp HD 116114 and Freyhammer et al. 2008b for a null-result for HD 151878). Freyhammer et al. (2008a) excluded rapid oscillations for 9 luminous Ap stars to high precision, so it may be particularly difficult to detect roAp stars among the sample here.

Projected rotation velocities (also in Table 2) were determined from the widths of the two Fe I lines  $\lambda 5434.52$  Å and  $6586.69$  Å that are rather insensitive to magnetic broadening. A few rotational standards observed in the 2007 February run and some available UVES spectra of a few roAp stars with known rotation velocities were used as references for a FWHM– $v \sin i$  relation. These velocities were verified during the SYNTHMAG analysis (Sect. 3.2.2), and found to agree within  $\pm 1$  km s<sup>-1</sup>.

### 3.2.2 Abundance estimates

For the purpose of evaluating the level of chemical peculiarities and ionization disequilibria, we made simple abundance estimates of Fe, Cr, Nd, Pr and Eu. Synthetic spectra were produced with SYNTHMAG (Piskunov 1999) for  $\log g = 4.0$  and 4.5, and the measured magnetic field strengths and photometric temperatures and then compared to the observed spectra for a range of Cr, Fe, Nd, Pr, Eu abundances. Because of the strong magnetic fields, we used model atmospheres from the online grid<sup>3</sup> by Castelli & Kurucz (2003) calculated with the ATLAS9 code with  $\xi = 2$  km s<sup>-1</sup> pseudo-microturbulence in order to simulate effects from magnetic intensification of spectral lines. Model atmospheres with increased solar metal abundance  $\log(N_{\text{Z}}/N_{\text{Z},\odot}) = +0.5$  were used. For spectrum synthesis for the magnetic stars, we used  $\xi = 1$  km s<sup>-1</sup> as the SYNTHMAG code includes magnetic intensification by directly including magnetic field effects. This value is slightly conservative, but is based on values used

by other studies in the literature for magnetic Ap stars (such as 1–4 km s<sup>-1</sup> for 1–9 kG fields: Ryabchikova et al. 2006b, 2007; Cowley & Hubrig 2008).

Atomic line data were taken from the VALD database using increased rare earth element abundances (identical for all models). The grid of models had  $7000 \leq T_{\text{eff}} \leq 9500$  K according to the photometric temperatures in Table 2, in steps of 500 K. Abundances were computed in steps of 0.1–0.5 dex but optimised on a case-by-case basis. The simplified SYNTHMAG model of magnetic fields is characterised by three components: radial field  $B_r$  (field component parallel to the line of sight), meridional  $B_m$  (field component parallel to the surface at every surface point in the plane-parallel atmosphere) and longitudinal component  $B_l$  (assumed zero, as is justified for the plane-parallel approximation). For simplicity, magnetic fields were assumed to be combinations of equally strong radial and meridional fields based on the magnetic modulus values in Table 2. In a few cases, a longitudinal field was used instead of the meridional field. Abundances of Fe, Cr, Nd, Pr and Eu were varied in ranges corresponding to those found by Adelman (1973) in his study of 21 cool Ap stars. Instrumental broadening of  $0.05$  Å was adopted throughout, while  $1 - 6$  km s<sup>-1</sup> macroturbulence was used to optimise the fitting of observed spectra with model spectra on a star-by-star basis. Surface gravity of  $\log g = 4.0$  was assumed, except for HD 42075, HD 55540, HD 75049 and HD 121661 where  $\log g = 4.5$  was used.

Because of strong line blending, the common presence of unidentified lines in Ap spectra, and a typical  $S/N \sim 200$  of our spectra, it is not always easy to identify continuum regions around spectral lines to be used in the abundance analysis. Therefore, rather than rely on equivalent width measurements, we directly compared the synthetic spectra with the observed ones, evaluating the best agreement by eye. The microturbulence velocity was fixed to  $\xi = 1$  km s<sup>-1</sup> throughout, which meant that weak lines in some cases gave different abundances from stronger lines. However, by combining several lines of each element an ionization agreement within 0.2–0.5 dex ( $1\sigma$ ) was reached. This error is comparable to that introduced by not using the appropriate values of surface gravity in each stellar case and is acceptable for the present characterisation of the stars to demonstrate abundance variations. Comparison with the relative estimates for HD 92499 by Hubrig & Nesvacil (2007) shows reasonable agreement within the errors (differences may be explained by a possible inhomogeneous chemical surface distribution).

Further limitations of our simple analysis include: sensitivity of the derived abundances to errors of the photometric temperature estimates (we find, e.g., that  $\pm 250$  K may correspond to 2–33 per cent differences in equivalent width for the elements in Table 3, worst for Pr); and choice of microturbulence  $\xi$  for which a change of 1 km s<sup>-1</sup> may infer a change in abundances comparable to their stated errors (especially Nd, see, e.g., Cowley et al. 2000).

Conventionally, microturbulent motions are those with characteristic lengths that are small compared to the mean free path of a photon. The value of  $\xi$  is normally increased to simulate the effect of a strong magnetic field (magnetic intensification), but also chemical stratification (which may dominate the errors of our relative abundances by increasing the differences in abundance yields from weak and strong lines) produces effects adverse to microturbulence. Because

<sup>3</sup> Available at <http://kurucz.harvard.edu>

of horizontal inhomogeneities and vertical stratification of the studied sample of magnetic Ap stars, abundance analysis is a demanding task (see examples of such studies in the Introduction) and is outside the aim of the present discovery paper. We are here interested in relative abundances to verify peculiar abundances and different abundances between elements of different ionization states. For this purpose, the estimated abundance errors of 0.2 – 0.5 dex are acceptable.

Table 3 gives the relative abundances found, and comments on the individual stars are given in Sect. 3.3. We used 30–70 lines of the 5 elements per star, but the actual selection of lines varied from star to star. Note that the models used for HD 135728 had the simplifying assumption of a combined continuum of two similar stars (with the same luminosity and spectral type). In their study of spectroscopic signatures of roAp stars, Ryabchikova et al. (2004) note the following Pr and Nd anomalies, expressed as differences in  $\log(N/N_{\text{tot}})$  of second and first ionized states, for roAp stars (further including the recent roAp discoveries HD 116114 and HD 137909)  $\Delta[\text{Pr}]_{\text{III-II}} = -0.22$  to 2.19 and  $\Delta[\text{Nd}]_{\text{III-II}} = 0.14$  to 2.55. For other Ap stars, the anomalies appear smaller with corresponding ranges  $\Delta[\text{Pr}]_{\text{III-II}} = -0.51$  to 1.38 and  $\Delta[\text{Nd}]_{\text{III-II}} = -0.36$  to 1.98. The authors thus suggest that roAp stars may have abundance differences for the first two ionized states of Pr and Nd of at least 1.5 dex and up to 2.5 dex, while non-pulsating stars show marginal differences. Only 4 stars in Table 3 had clear indications of ionization disequilibria for both Pr and Nd. These stars are HD 44226, HD 92499 (as already found by Hubrig & Nesvacil 2007), HD 96237 and HD 143487 and they are therefore promising roAp star candidates. Furthermore, HD 33629, HD 42075 and HD 69013 have significantly different abundances for Nd II and Nd III, though the same is not clear for Pr. Si II 6347 Å and 6371 Å are strong in all spectra, and even prominent in most except for HD 69013, HD 96237 and HD 143487.

### 3.2.3 Magnetic field measurements

A strong field, typically  $\sim 2 - 3$  kG, combined with a slow projected rotation rate (smaller than  $v \sin i \sim 10 \text{ km s}^{-1}$ ) can produce magnetically resolved lines by the Zeeman effect (Mathys et al. 1997). In the simplest cases of spectral lines corresponding to doublet or triplet Zeeman patterns, simple formulae can be applied to determine in a virtually approximation-free manner the mean magnetic field modulus  $\langle B \rangle$  from measurement of the wavelength separation of the resolved Zeeman components (Mathys 1989).  $\langle B \rangle$  is the average of the modulus of the magnetic vector, over the visible stellar hemisphere, weighted by the local line intensity. For a triplet pattern, its value (in G) is obtained from the wavelength separation  $\Delta\lambda$ , between the central  $\pi$  component and either of the  $\sigma$  components, by using the formula:

$$\langle B \rangle = \Delta\lambda / (4.67 \cdot 10^{-13} \lambda_c^2 g_{\text{eff}}), \quad (1)$$

where  $\lambda_c$  is the central wavelength of the line and  $g_{\text{eff}}$  is the effective Landé factor of the transition. Both  $\Delta\lambda$  and  $\lambda_c$  are expressed in Å. For a doublet pattern, the relation between  $\langle B \rangle$  and the separation  $\Delta\lambda$  of the split components (each of which is the superposition of a  $\pi$  and a  $\sigma$  component) is:

$$\langle B \rangle = \Delta\lambda / (9.34 \cdot 10^{-13} \lambda_c^2 g_{\text{eff}}). \quad (2)$$

As shown in Fig. 1, the Zeeman splitting of the  $\lambda 6149$  Å line is visible for nearly all 18 stars in the FEROS spectra (HD 96237 excepted, see Sect. 3.3.13). The UVES follow-up observations (Fig. 2) showed considerable changes in this line for 4 stars: *HD 143487* which has only partially split lines in the FEROS spectrum; *HD 135728AB*, an SB2 binary; *HD 96237* which is highly variable and peculiar, and which showed magnetically resolved lines in the 2007 March spectrum only, and then only for a few Cr and Fe lines. The  $\lambda 6149$  Å line in this star is never seen as double, but appears broadened in the 2007 March observations (Fig. 2) to an extent that is in good agreement with a magnetic field modulus of 2.6 kG; and finally *HD 75049* which is an extremely magnetic star that shows, probably due to rotation, a changing magnetic field strength and spectral fine-structure, such as appearance and disappearance of the Paschen-Back effect in certain wavelength regions. The mean magnetic field modulus  $\langle B \rangle$  measurements based on  $\lambda 6149$  Å are given in Table 2. The corresponding errors are based on measurements repeated in different spectra when available. These errors may be affected by spectrum-to-spectrum variations in the magnetic field strength itself, related to the stellar rotation. Errors are also sensitive to conditions such as  $v \sin i$ , blends from close lines, and the magnetic field strength (i.e. how well separated the Zeeman components are). For 6 stars with only a single spectrum available, the errors were estimated based on  $v \sin i$ , and on errors found for stars with similar  $\lambda 6149$  Å line profile shapes, using as a lower limit the scatter from repeating the measurements using different settings for treating blends and continuum placement. Further details are given in Sect. 3.3.

Measurements of line broadening and of separation of Zeeman split components in magnetically resolved lines were made by using IRAF’s onedspec.plot task. For blended cases, 2–4 Gaussian profiles were fitted simultaneously and Eqs. 1 and 2 were applied to determine the mean magnetic modulus  $\langle B \rangle$ . The magnetic measurements were made mostly for the same set of lines, but due to differences in line broadening, magnetic splitting, differences in abundances resulting in different degrees of line blending, the choice of lines used was always made on a star-by-star basis. The most important lines used, with large Landé factors ( $g_{\text{eff}} = 1.2 - 2.9$ ), are: Cr I 5247.56 Å, Cr II 5116.04 and 6112.26 Å, Eu II 6437.64 Å, Fe I 5068.76, 6230.72, 6232.64, 5324.17 and 6336.82 Å, and Fe II 6149.25, 6369.46, 6383.72, 6446.41 and 6600.02 Å.

Spectra of the stars re-observed in 2007 March were used for checking radial velocity (RV) stability by measuring the two non-magnetically sensitive iron lines Fe I 5434.52 Å, Fe II 6586.69 Å and occasionally also Nd III 6145.63 Å. The wavelength scales in all cases have been added offsets determined from lines selected in the telluric line list by Griffin & Griffin (1973). This ensures accurate radial velocities to the level of  $300 \pm 200 \text{ m s}^{-1}$ , sufficient for first checks on duplicity for the considered interval of 30 – 35 d.

### 3.3 Individual notes

In this section individual magnetic stars are described in sequence of appearance in the Henry Draper Catalogue. Spectral classifications from the Michigan Spectral Catalogue are given in Table 3 and repeated here when individual notes from the Catalogue were available.

**Table 3.** Relative abundance estimates with number of lines used indicated (n). Estimated errors are 0.2 – 0.5 dex. Columns 11–12 give the abundance differences between the first two ionized states of Pr and Nd; significant ionization disequilibrium anomalies are indicated with bold font. Last column is the Michigan classification (Houk 1978, 1982; Houk & Cowley 1975; Houk & Smith-Moore 1988). The last row is for the solar atmosphere (Asplund, Grevesse & Sauval 2005).

HD	$\log(N/N_{\text{tot}})$												Class.								
	Cr I n	Cr II n	Fe I n	Fe II n	Pr II n	Pr III n	Nd II n	Nd III n	Eu II n	$\Delta[\text{Pr}]_{\text{III-II}}$	$\Delta[\text{Nd}]_{\text{III-II}}$										
33629	-5.60	3	-5.44	5	-4.29	16	-4.37	6	-8.57	4	-8.80	3	-8.96	8	-7.93	3	-9.68	3	-0.23	<b>1.03</b>	<i>*Ap SrCr(Eu)</i>
42075	-5.83	4	-5.68	6	-4.55	17	-4.24	7	-8.27	3	-8.23	4	-8.30	11	-7.00	2	-8.50	3	0.04	<b>1.30</b>	<i>*Ap EuCrSr</i>
44226	<-5	1	-4.53	4	-3.79	8	-4.09	7	<-9.8	2	-8.20	3	-8.37	4	-7.53	3	-8.95	2	> <b>1.60</b>	<b>0.84</b>	<i>*Ap SrEuCr</i>
46665	-5.55	6	-5.18	8	-4.99	15	-4.43	6	-8.80	2	-8.80	3	-8.17	17	-7.83	2	-9.27	3	0.00	0.34	<i>*Ap EuSrCr</i>
47009	-5.55	4	-5.73	4	-4.76	7	-4.52	6	-8.40	3	-9.13	3	-8.23	9	-8.20	3	-8.73	3	<b>-0.73</b>	0.03	<i>*Ap EuCr(Sr)</i>
52847	-3.60	4	-3.48	12	-4.24	14	-3.57	5	-9.13	4	-9.25	2	-8.30	6	-8.30	2	-7.57	3	-0.12	0.00	<i>*Ap CrEu(Sr)</i>
55540	-4.63	3	-3.92	13	-5.02	6	-4.34	7	-8.43	3	-8.48	5	-8.23	4	-8.30	2	-8.90	3	-0.05	-0.07	<i>*Ap EuCr</i>
69013	-6.10	3	-5.50	5	-4.71	15	-4.70	5	-7.45	3	-8.33	3	-8.34	21	-7.10	3	-9.15	3	<b>-0.88</b>	<b>1.24</b>	<i>*Ap EuSr</i>
72316	-4.83	4	-4.70	13	-4.59	16	-4.09	9	-9.90	2	-9.45	4	-8.55	7	-8.65	2	-9.23	3	0.45	-0.10	<i>*Ap EuCr(Sr)</i>
75049	-4.70	1	-4.56	7	-4.30	5	-4.04	11	-8.50	1	-8.25	4	-7.65	2	-7.45	2	-7.80	3	0.25	0.20	<i>*Ap EuCr</i>
88701	-4.81	8	-4.34	20	-4.96	16	-4.01	8	-8.50	3	-8.95	6	-8.62	9	-8.75	2	-8.90	3	-0.45	-0.13	<i>*Ap CrSi</i>
92499	-5.90	4	-4.93	3	-4.59	12	-4.35	6	-8.70	3	-8.20	3	-8.08	18	-6.83	4	-9.30	3	<b>0.50</b>	<b>1.25</b>	<i>*Ap SrEuCr</i>
96237 <sub>φ1</sub>	-5.84	5	-5.10	6	-4.71	9	-4.71	5	-8.28	5	-7.64	5	-6.80	17	-5.60	3	-9.85	3	<b>0.64</b>	<b>1.20</b>	<i>*Ap SrEuCr</i>
96237 <sub>φ2</sub>	-4.98	4	-4.72	5	-4.24	8	-4.15	3	-9.55	2	-8.23	4	-8.72	5	-6.43	3	-8.73	3	<b>1.32</b>	<b>2.29</b>	
110274	-4.89	7	-4.58	19	-4.57	17	-4.25	10	-9.23	4	-9.02	5	-8.77	13	-8.20	2	-8.63	3	0.21	<b>0.57</b>	<i>*Ap EuCr</i>
117290	-5.08	6	-4.78	11	-4.33	17	-4.28	13	-9.18	4	-9.30	3	-8.89	10	-8.80	5	-8.67	3	-0.12	0.09	<i>*Ap EuCrSr</i>
121661	-5.10	3	-4.25	5	-4.52	10	-3.98	4	-8.97	3	-8.78	3	-8.14	7	-7.88	2	-8.97	3	0.19	0.26	<i>*Ap EuCr(Sr)</i>
135728A			-5.67	4	-3.36	5	-3.35	6	<-10.50	2	-10.20	2	-8.70	4	-8.70	2	-9.40	2	>0.23	-0.24	<i>*Ap SrEuCr</i>
135728B	-4.48	3	-4.47	9	-4.30	5	-4.30	3	-8.83	3	-9.13	4	-8.31	8	-8.10	2	-8.80	2	0.07	-0.03	
143487	-5.50	3	-5.33	8	-5.09	9	-4.70	9	-9.20	3	-7.70	2	-8.08	11	-6.72	5	-8.60	2	<b>1.50</b>	<b>1.36</b>	<i>*APEC</i>
Sun	-6.40		-6.40		-4.59		-4.59		-11.33		-11.33		-10.59		-10.59		-11.52				

To supplement the  $\lambda 6149 \text{ \AA}$  measurements in Table 2, Zeeman measurements for other lines are also given. However, while  $\lambda 6149 \text{ \AA}$  is a heavily used diagnostic line for which the blending is rather well known, interpretation of the field strengths measured for other lines, especially of different chemical elements, is not straightforward. This in part because the Landé factors of different lines not always have the same reliability, but more importantly because blending of other (non-diagnostic) lines may be much less secure. Furthermore, lines of elements such as Cr or REEs may have differences in their distribution over the stellar surface, meaning that the field measurement is weighed differently. Differences between field values from lines of different elements thus result in a scatter that is larger than for  $\lambda 6149 \text{ \AA}$  alone based on more spectra. Most likely it reflects actual physical effects in the star, rather than provides a reliable estimate of the measurement errors.

### 3.3.1 HD 33629

From the magnetic components of  $\lambda 6149 \text{ \AA}$  we measure a magnetic field of  $4.76 \pm 0.17 \text{ kG}$ , which combined with the measurements of  $\text{Fe I } 6232.64 \text{ \AA}$  and  $\text{Fe II } 6369.46 \text{ \AA}$  gives  $\langle B \rangle = 4.21 \pm 0.48 \text{ kG}$ . The photometric temperature is  $T_{\text{eff}} = 7570 \text{ K}$ . The abundance estimates in Table 3 show overabundances of Nd, Pr, Eu and Cr compared to the Sun, a solar Fe abundance, and ionization disequilibrium for Nd only. The line  $\text{Ba II } 6141.71 \text{ \AA}$ , common in many roAp stars, is very strong. The ASAS photometry excludes rotational photometric variability greater than 5.1 mmag amplitude.

### 3.3.2 HD 42075

Observed on three different nights (see Table 1), this star had a constant radial velocity  $4.2 \pm 0.4 \text{ km s}^{-1}$ . From the resolved  $\lambda 6149 \text{ \AA}$  line, all spectra give  $\langle B \rangle = 8.54 \pm 0.02 \text{ kG}$  which with Zeeman splitting measured for 6 additional iron lines shows a stable magnetic field of  $8.58 \pm 0.14 \text{ kG}$  for all nights combined. ASAS photometry indicates no variability above 4.0 mmag. The star's sharp-lined spectrum ( $v \sin i \sim 1 \text{ km s}^{-1}$ ) adds further support to a slow rotation period, longer than a month. The abundance estimates in Table 3 show overabundances of Cr, Pr, Nd and Eu, and near-solar Fe.  $\text{Ba II } 6141.71 \text{ \AA}$  is very strong (see also Figs. A1 and A2).

### 3.3.3 HD 44226

The  $\lambda 6149 \text{ \AA}$  line indicates  $\langle B \rangle = 4.99 \pm 0.01 \text{ kG}$  which with  $\text{Fe I } 6232.64 \text{ \AA}$  and  $\text{Fe II } 6369.46 \text{ \AA}$  combined gives  $\langle B \rangle = 5.04 \pm 0.52 \text{ kG}$ . ASAS photometry excludes periodic variability above 5.3 mmag. The spectrum is similar to that of HD 33629 and also shows a very strong  $\text{Ba II } 6141.71 \text{ \AA}$  line. All abundances in Table 3 are greater than solar. As ionization disequilibria for both Nd and Pr are similar to those of known roAp stars,  $\Delta[\text{Pr}]_{\text{III-II}} \geq 1.60$  and  $\Delta[\text{Nd}]_{\text{III-II}} = 0.84$ , this star is a good roAp candidate.

### 3.3.4 HD 46665

This star shows no long-period photometric variability above 5.1 mmag in  $V$  (from the ASAS survey). Our two spectra obtained 35 d apart indicate an unchanged radial velocity,  $22.9 \pm 0.2 \text{ km s}^{-1}$ . The magnetic measurements for  $\lambda 6149 \text{ \AA}$  give similar values, 4.72 and 4.53 kG, or  $\langle B \rangle = 4.63 \pm 0.13 \text{ kG}$

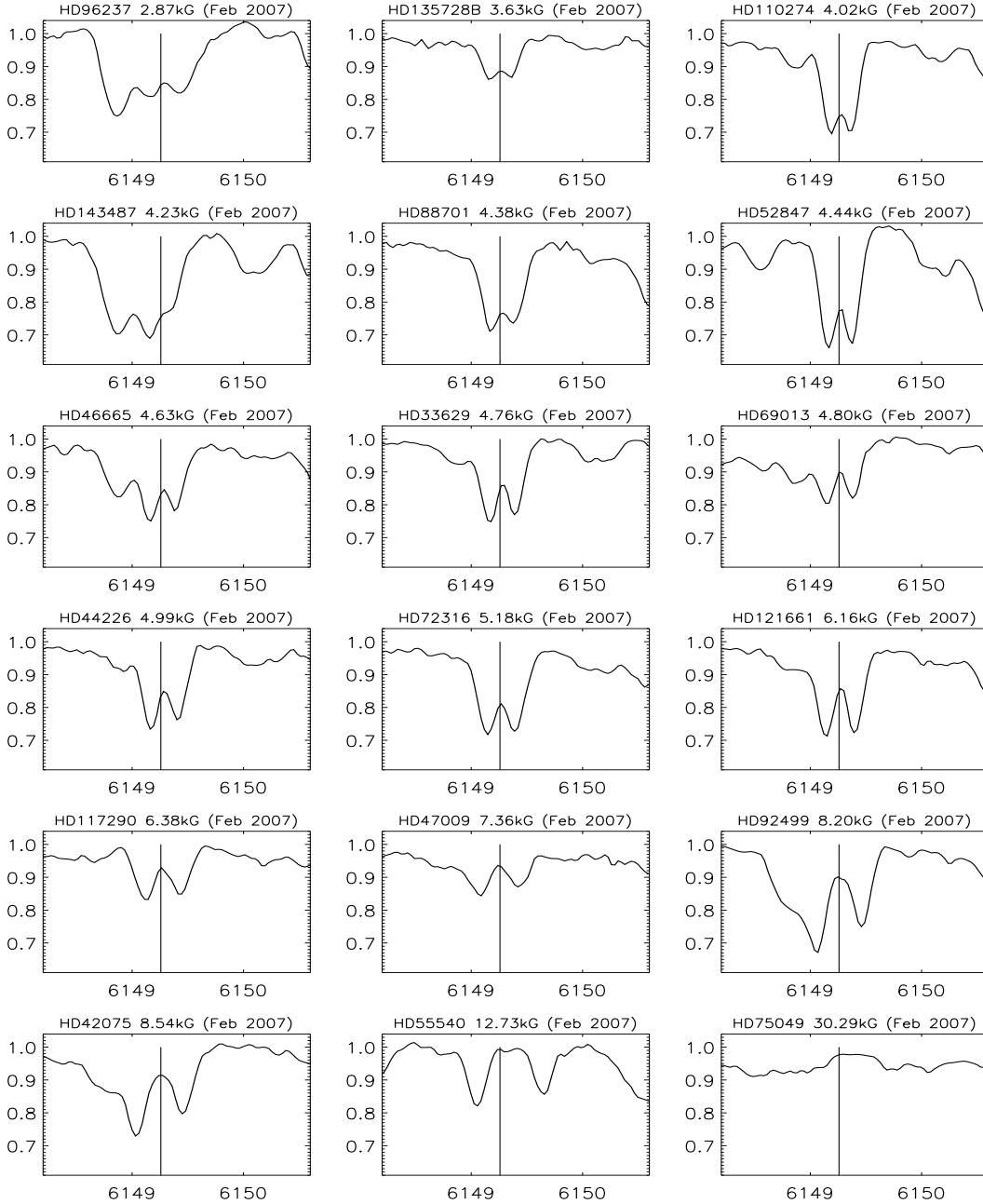


**Figure 1.** Comparison of the magnetically resolved Fe II 6149 Å lines in the 2007 February (FEROS) spectra. The abscissa is wavelength in Å, the ordinate is normalized intensity. Radial velocity shifts were added to the laboratory wavelengths estimated from H $\alpha$ . Note that for HD 96237, the region with  $\lambda$ 6149 Å is dominated by unidentified rare earth elements as iron is particularly weak at this rotation phase (Table 3). The spectra appear from top (left) to bottom (right) with increasing magnetic field modulus ( $B$ ) from Table 2.

combined. This is supported by including an additional 2–3 Cr and Fe lines which give  $4.64 \pm 0.23$  and  $4.68 \pm 0.13$  kG for the FEROS and UVES spectra respectively. The spectrum shows an absence of barium (especially  $\lambda$ 6141 Å) and lines of silicon are weak. Overabundances of Cr, Nd, Pr and Eu are found, while the Fe abundance is solar. The Michigan Catalogue classification and note is *\*ApEuSrCr, or possibly Si rather than Eu; this is the strongest of the metal lines, but note that we find weak Si in our recent spectra.*

### 3.3.5 HD 47009

The  $\lambda$ 6149 Å line indicates a field strength of  $7.36 \pm 0.13$  kG, confirmed by adding measurements for two more Cr and Fe lines which gives  $7.49 \pm 0.19$  kG. Photometrically, the star is stable to 4.1 mmag in  $V$ . The temperature is at the high end of our sample,  $T_{\text{eff}} = 8280$  K, as supported by the spectra. Long stretches of continuum are seen. Ba is absent, while Si and Ca are clearly present. Cr, Nd, Pr and Eu are greater than solar, while Fe is solar.



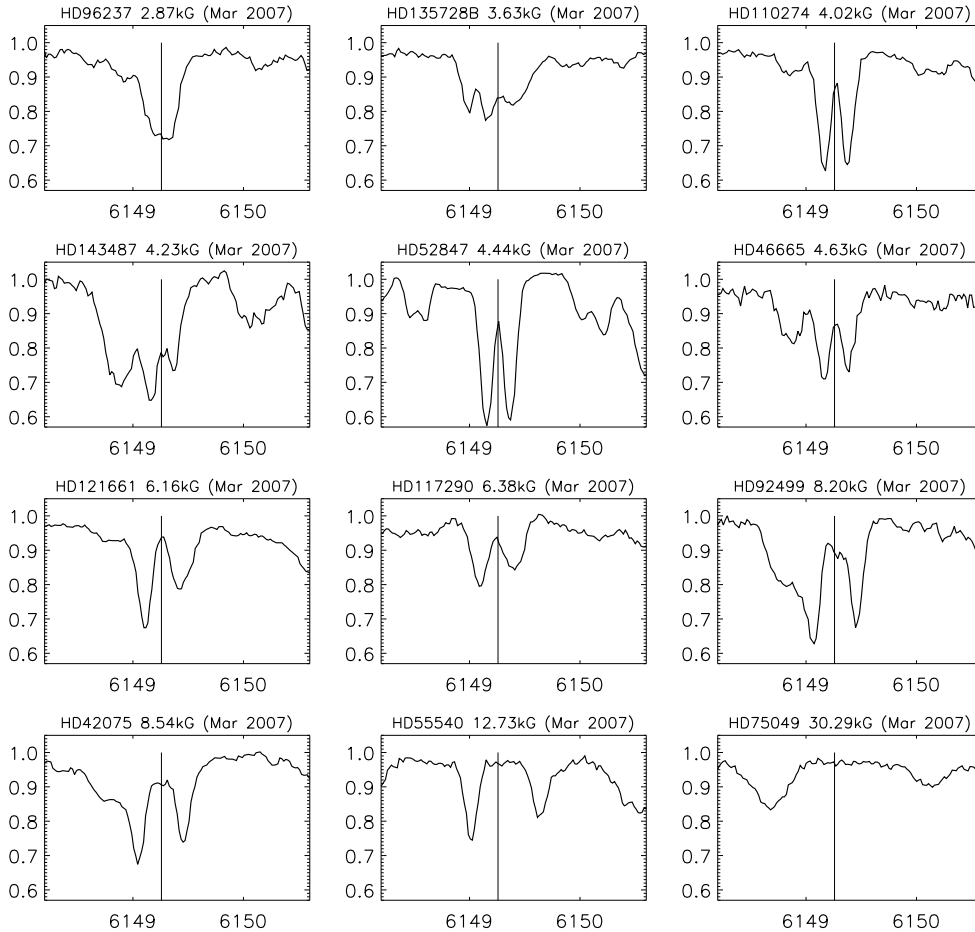


Figure 2. Same as Fig. 1, but for UVES spectra obtained about 1 month later for some of the stars.

### 3.3.6 HD 52847

Hensberge et al. (1984) found this star to be photometrically stable in Strömgren  $u$  to less than 15 mmag, which the ASAS  $V$  photometry confirms to 4.2 mmag. We obtained two spectra of the star, 35 d apart, both with the same radial velocity within the errors,  $11.3 \text{ km s}^{-1}$ . The Fe II 6149 Å line gives a constant magnetic field of  $4.44 \pm 0.01 \text{ kG}$  for both spectra, while adding 2 – 5 more Cr, Fe and Eu lines to the analysis confirms this result as  $\langle B \rangle = 4.76 \pm 0.61$  (HJD 2454138) and  $\langle B \rangle = 4.48 \pm 0.15 \text{ kG}$  (HJD 2454173). Note the considerable error compared to that of the *diagnostic* Fe II 6149 Å line, because of the effects mentioned in the beginning of Sect. 3.3. Of the studied stars, we find this star has the highest abundance of Cr, while Fe is near-solar and Nd, Pr and Eu are greater than solar. Ca is weak (Ca II K is sharp, corresponding to spectral type early A). Ba  $\lambda 6141 \text{ Å}$  is strong and Eu has the highest abundance of the studied stars.

### 3.3.7 HD 55540

Based on 15 single nightly measurements obtained over some years, Hensberge et al. (1984) claimed this star to be a long period variable with a 44 mmag variability in the Strömgren  $u$  band, at the  $2.5\text{-}\sigma$  level. However, the ASAS  $V$  band shows stability to 5.2 mmag over 5.6 years, at which amplitude a candidate period of 42.1 d is found. The signifi-

cance is marginal,  $4.2\sigma$ , but without *Hipparcos* photometry it is not a reliable detection. As a strong magnetic field was obvious in this star’s spectrum (12.5 kG), we observed it on 4 different nights in 2007 February and March. The three 2007 February spectra show similar radial velocity,  $RV = 49.9 - 50.5 \text{ km s}^{-1}$ , while the 2007 March spectrum exhibits a significantly lower velocity,  $RV = 36.6 \text{ km s}^{-1}$ . With typical radial velocity errors of  $0.5 - 0.8 \text{ km s}^{-1}$ , this is an unconfirmed detection of a radial velocity variable and probable SB1 binary. No indication of a secondary spectrum was noted. From Zeeman splitting measurements based on 5 – 7 Cr, Nd, Eu and Fe lines, we find that the magnetic field is slightly, but significantly, increasing:  $\langle B \rangle = 12.38 \pm 0.13$  (HJD 2454138),  $\langle B \rangle = 12.29 \pm 0.26$  (HJD 2454139),  $\langle B \rangle = 12.40 \pm 0.21$  (HJD 2454141) and  $\langle B \rangle = 13.04 \pm 0.21 \text{ kG}$  (HJD 2454173). The corresponding individual Fe II 6149 Å measurements give respectively  $\langle B \rangle = 12.50, 12.50, 12.63$  and  $13.07 \text{ kG}$  ( $\langle B \rangle = 12.73 \pm 0.30 \text{ kG}$ , combined). Cr, Nd, Pr and Eu are greater than solar and Fe is near-solar, and Ba  $\lambda 6141 \text{ Å}$  is present. The temperature (8280 K) is high for known roAp stars.

### 3.3.8 HD 69013

The  $\lambda 6149 \text{ Å}$  line indicates a magnetic field strength of  $4.80 \pm 0.06 \text{ kG}$ . When combining this line with two more iron lines and Eu II 6437.64 Å (only partially split), a field of  $\langle B \rangle =$

$4.33 \pm 0.39$  kG is determined. There is no variability seen with the ASAS photometry to 4.1 mmag for this relatively faint star ( $V = 9^m45$ ). Cr and Fe abundances are near-solar and solar, respectively, while abundances of Nd and Pr are some of the highest in this study. Eu is also greater than solar. The Ba, Ca and Si lines are all prominent. Nd and Pr ionization disequilibrium anomalies of  $\sim 1$  dex are found in opposite directions, which is not seen in known roAp stars.

### 3.3.9 HD 72316

Based on  $\lambda 6149 \text{ \AA}$ , a field of  $\langle B \rangle = 5.18 \pm 0.33$  kG is found. This is confirmed with the Cr II lines  $\lambda\lambda 5116.05 \text{ \AA}$  and  $5318.38 \text{ \AA}$  which indicate  $\langle B \rangle = 5 - 6$  kG. ASAS photometry shows no variability above 4.5 mmag. Si I and Ca are weak and barely visible. A sharp Ca II K line supports the photometric temperature of  $T_{\text{eff}} = 8050$  K (early to mid-A type). Ba  $\lambda 6141 \text{ \AA}$  is present ( $\sim 4$  per cent absorption below continuum). All Cr, Fe, Nd, Pr and Eu abundances are greater than solar, but Nd, Pr and Eu have some of the lowest abundances in the studied sample of stars. In the astrometric H-R diagram, the star appears to be near the end of its main sequence lifetime.

### 3.3.10 HD 75049

This star has the second strongest magnetic field of all known Ap stars, and if this field is variable, it may even surpass that of HD 215441 (34.4 kG, Babcock 1960) at some phases. Our spectra, separated by 30 d, show considerable differences in the field strength and component fine-structure (Fig. 3) probably related with viewing different aspects of the star's magnetic field and surface element distribution. The strength of the field is such that the splitting pattern of the  $\lambda 6149 \text{ \AA}$  line is strongly distorted by partial Paschen-Back effect, hampering its use as a diagnostic line. The splitting observed in the 2007 February spectrum cannot be simply interpreted, while the appearance of the line in the 2007 March spectrum is more similar to the doublet pattern observed in stars with weaker fields. If the separation of the two components is translated to a magnetic field in the usual manner, a value of  $\langle B \rangle = 30.29 \pm 0.08$  kG is obtained for this epoch. However, application of Eq. (2) in this case is not quite justified. Combining the Fe II  $6149 \text{ \AA}$  measurement with those of an additional 4 Nd, Eu and Fe lines we obtain  $\langle B \rangle = 30.33 \pm 0.48$  kG.

The 2007 February spectrum's lower resolution, together with the partial Paschen-Back effect, limits the number of resolved lines available for magnetic field measurements. With a few lines, Nd III  $6145.07 \text{ \AA}$ , Nd III  $6550.32 \text{ \AA}$  and Fe II  $6456.38 \text{ \AA}$ , a field of  $\langle B \rangle = 25.77 \pm 1.81$  kG is obtained. Radial velocity measurements ( $10.2 \pm 0.6 \text{ km s}^{-1}$ , combined) show no differences for the two spectra above  $1.0 \text{ km s}^{-1}$ , which is within the measurement errors.

The ASAS photometry reveals (Fig. 4) the star to be an  $\alpha^2$  CVn rotational variable with two significant periodicities: 5.28 yr (12.7 mmag amplitude,  $7.4 \sigma$ ) and a much shorter one at 4.05 d (7.9 mmag,  $5.5 \sigma$ ). As the spectra show considerable variability in just 30 d, and  $v \sin i = 8 \text{ km s}^{-1}$ , we suspect that the shorter period may be identified as the rotation period. The epochs in Table 1 show that our two spectra were

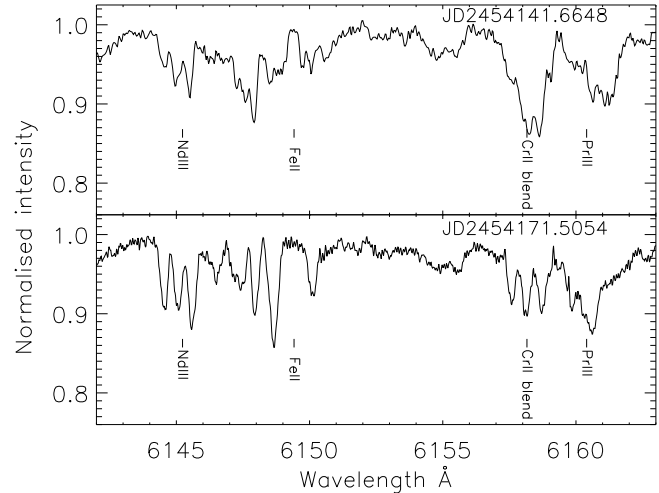


**Figure 3.** A portion of the spectrum of HD 75049 recorded with FEROS on 2007 February 10 (top), and with UVES on 2007 March 11 (bottom). Very significant variations of the spectral line intensities and shapes between the two epochs are clearly seen.

taken 7.4 rotation cycles apart for the 4.05-d rotation period. This is consistent with the observed spectral variability.

From the shape of the H $\alpha$  wings and from the photometric temperature estimate, the temperature of this Ap star is  $T_{\text{eff}} = 9700$  K, in excellent agreement with the weak and sharp Ca II K line that indicate A0 or even late-B type. Ba, Si I and Ca are weak or not visible. (Ba  $\lambda 6141 \text{ \AA}$  is present but broadened or scrambled, weak and asymmetric). Cr, Nd, Pr and Eu have greater than solar abundances, while Fe is solar or near-solar. No Nd or Pr ionization anomalies are found. We are currently performing follow-up with spectroscopy and spectropolarimetry to establish the rotation rate, mean magnetic field modulus and mean longitudinal field to characterise HD 75049's magnetic and spectral variations and derive a first model of its magnetic field. The spectral classification from the Michigan Catalogue with a note is *\*ApEuCr*. Or very possibly *Si* rather than *Eu*.

### 3.3.11 HD 88701

The  $\lambda 6149 \text{ \AA}$  line indicates a field of  $\langle B \rangle = 4.38 \pm 0.32$  kG. With 3 additional Cr and Fe lines, we get  $\langle B \rangle = 4.21 \pm 0.41$  kG. Ba, Ca and Si I are weak or absent, while Cr, Pr, Nd and Eu are greater than solar. Although Fe appears to differ in abundances of its two ions, the mean abundance is solar. A sharp Ca II K line indicates early-A type, while our photometric temperature estimate is  $T_{\text{eff}} = 8080$  K. The ASAS V light curve shows (Fig. 5) a double-wave when phased with the period 25.765 d. This is a clear  $\alpha^2$  CVn signature of a spotted surface and as  $v \sin i = 7 \text{ km s}^{-1}$  is one of the highest of our sample, we identify the period as the rotation period. If we take the rotation period and measured  $v \sin i$  at face value, the implication is that HD 88701 has a radius of  $R = 3.5 R_{\odot}$ , an unexpectedly high value. However, with an error estimate of  $\pm 1 \text{ km s}^{-1}$ , a  $3 \sigma$  lower limit on  $v \sin i$  of  $4 \text{ km s}^{-1}$  then leads to a much more typical radius for magnetic Ap stars of  $2 R_{\odot}$ . These numbers suggest that the rotational inclination is close to  $90^\circ$ . The spectral classifica-

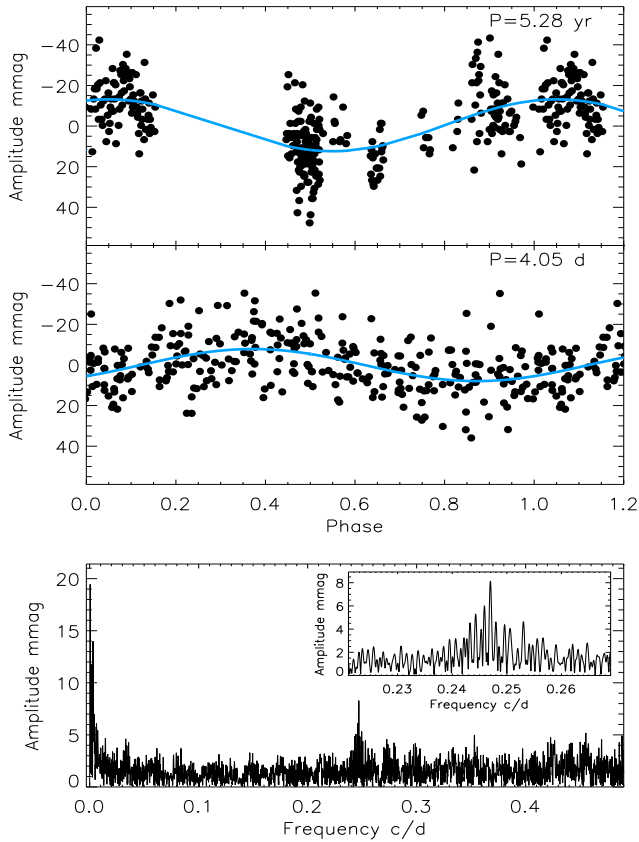


**Figure 4.** Upper panel: ASAS light curve of HD 75049 folded with the dominant 5.28 yr-period. The data were observed in the shown sequence. Middle panel: the same light curve with the 5.28 yr period prewhitened and folded with the 4.05 d period. Best-fit models are superposed the light curves. Lower panel: The corresponding amplitude spectra showing the 5.28 yr-period with the second period at 4.05 d; the insert is a zoom-in on the latter period, after prewhitening for the former. Note the smaller amplitude scale.

tion from the Michigan Catalogue with a note is *\*Ap CrSi. Fairly weak but definite case.*

### 3.3.12 HD 92499

This Ap star was recently discovered to have magnetically resolved lines by Hubrig & Nesvacil (2007), who on 2006 May 13 observed the star and measured  $\langle B \rangle = 8.5 \pm 0.2$  kG and  $v \sin i = 3.0 \pm 0.5$  km s $^{-1}$ . We re-observed the star on 4 different nights. Using 7 Fe lines for the FEROS spectra and 20 for the UVES spectrum, we measured:  $\langle B \rangle = 8.12 \pm 0.17$  (HJD2454138),  $8.06 \pm 0.27$  (HJD2454139),  $8.17 \pm 0.12$  (HJD2454141) and  $8.09 \pm 0.31$  kG (HJD2454172), i.e. a constant field strength, slightly smaller than Hubrig et al.’s measurement. Of these Fe line measurements, the  $\lambda 6149$  Å line alone shows no trends and provides, combined for all 4 spectra,  $\langle B \rangle = 8.20 \pm 0.13$  kG. Radial velocities of all spectra show no variability with  $RV = 18.39 \pm 0.25$  km s $^{-1}$ . The ASAS light curve (Fig. 6) shows a 40 mmag increase in 3.7 yr, while the *Hipparcos* data (separated from the ASAS data by  $\sim 7.5$  yr) show no change above 9.8 mmag in 3.2 yr, but this could occur during light curve maximum or minimum. If

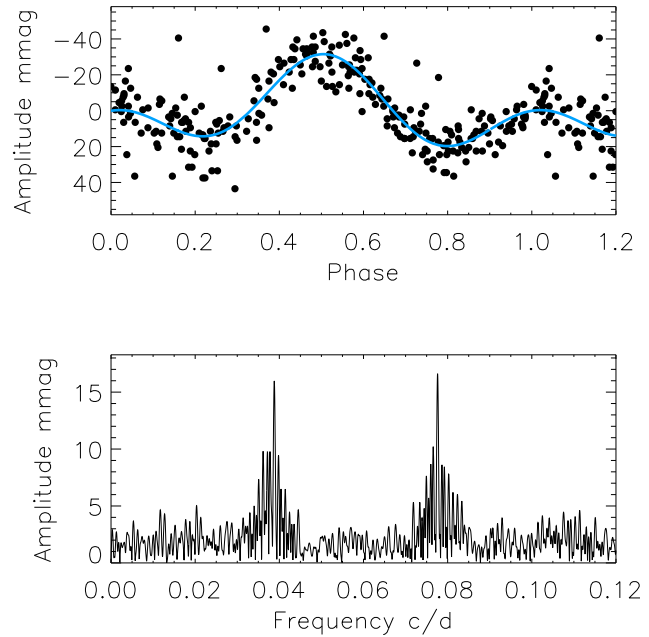


**Figure 5.** Top: ASAS light curve of HD 88701 folded with the rotation period 25.765 d and the best-fit model superimposed. The double-wave is characteristic for  $\alpha^2$  CVn variables.

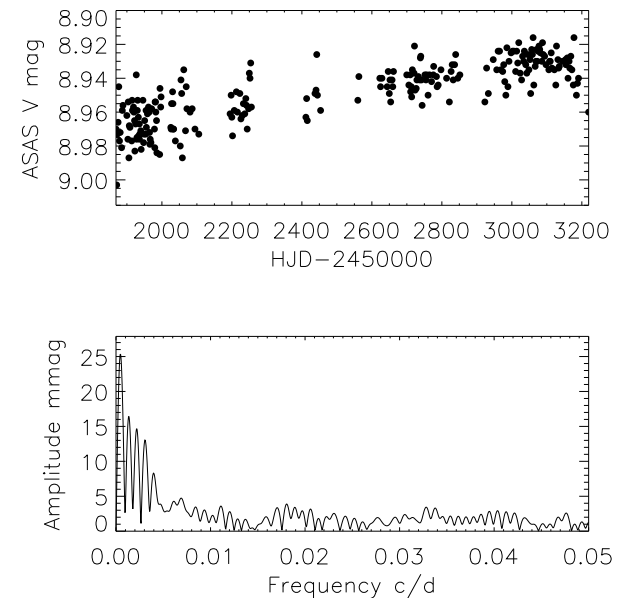


**Figure 6.** ASAS light curve of HD 92499 covering a period of 3.7 yr. Below is the corresponding amplitude spectrum.

the ASAS variability is real and related to the rotation, a rotation period longer than 5 yr would be expected.

The abundances of Cr, Pr, Nd and Eu are greater than solar; Fe is near-solar. Ba  $\lambda 6141$  Å is present but very shallow. The Ca II K line suggests type late-A to early-F which makes the photometric temperature of  $T_{\text{eff}} = 7810$  K seem slightly high. As found by Hubrig & Nesvacil (2007), we see Pr and Nd ionization anomalies:  $\Delta[\text{Pr}]_{\text{III-IV}} = 0.50$  and  $\Delta[\text{Nd}]_{\text{III-IV}} = 1.25$ . This star is a promising roAp candidate.

3.3.13 *HD 96237*

This star is enigmatic and intriguing. It is best described as a highly peculiar, magnetic Ap star with a spectrum that changes dramatically in the 1-month time span of our observations. We obtained two spectra of the star, 35 d apart in time, and at first sight they appear to be two different stars (see upper two spectra in Figs. 7 and 8). This is, however, not the case. Radial velocity measurements give the same velocity,  $1.4 \text{ km s}^{-1}$ , within  $340 \text{ m s}^{-1}$ . As shown in the figure, the overall shape of  $H\alpha$  is similar, considering the  $\sim 4$  per cent uncertainty in the normalisation of this region of the UVES spectrum (two orders merge here), and a possibly very inhomogeneous surface distribution of elements. An 8000 K model spectrum fits the  $H\alpha$  wings best in the 2007 February spectrum, and a slightly cooler ( $\sim 200 \text{ K}$ ) model spectrum of about 7800 K fits the  $H\alpha$  wings better in the 2007 March spectrum. Both temperatures agree well with the late-A spectral type indicated by the shape of the  $\text{Ca II K}$ -line profile. The stable radial velocity and single  $H\alpha$  line (also other hydrogen lines and calcium lines in the FEROS spectrum are single) give no evidence of a secondary spectrum. The 2007 March spectrum was recorded during evening twilight at an air mass of 1.8, but line contamination from the solar spectrum is excluded as the reason for the difference from the 2007 February spectrum.

The star is a known photometric variable listed as  $\alpha^2 \text{ CVn}$  in the General Catalog of Variable Stars (GCVS4.2, Samus, Durlevich, & et al. 2004), and as a semi-detached eclipsing binary in the ASAS catalogue. Period analysis of the ASAS light curve confirms a variability (Fig. 9), which we interpret as a single-wave  $\alpha^2 \text{ CVn}$  periodicity of 20.91 d with an amplitude of 49 mmag. As demonstrated in Fig. 9, the fit is improved by including the first harmonic at  $0.0956 \text{ cd}^{-1}$  which is detected at the  $4.4 \sigma$  significance level. The *Hipparcos* light curve confirms the 20.91 d period. Assuming this to be the rotation period (we cannot rule out a double-wave light curve with a 41.83 d rotation period) it agrees well with the short timescale between the two epochs of our recorded spectra, during which the abundances have changed. The spectrum variability is exceptional among known Ap stars, and the very peculiar line strengths in the 2007 February spectrum resemble those of the most peculiar Ap star known, HD 101065 (Figs. 7 and 8). That latter star has, however, a rotation velocity close to zero, which makes HD 96237 of particular interest for studying the chemical surface distribution in 2-D.

HD 96237 now joins the small group of extreme Lanthanide Ap stars that includes HD 51418 (Jones et al. 1974) and the more famous HR 465 (HD 9996; Preston & Wolff 1970), as well as HD 101065. These other stars have comparable magnetic field strengths: HD 101065 has partially resolved Zeeman components giving a magnetic field modulus of  $\langle B \rangle = 2.30 \pm 0.35 \text{ kG}$  (Cowley et al. 2000) in agreement with  $\langle B \rangle = 2.3 \text{ kG}$  measured by us using UVES spectra and based on a partially resolved Zeeman pattern in the  $\text{Gd II } 5749 \text{ \AA}$  line; HD 51418 has a mean longitudinal magnetic field which varies from  $\langle B_z \rangle = -200$  to  $750 \text{ G}$  (Jones et al. 1974); and HR 465 has  $\langle B \rangle = 4.83 \pm 0.39 \text{ kG}$  (Mathys et al. 1997). HD 51418 has a rotation period of 5.4379 d, typical of the Ap stars, but HR 465 is known for its long rotation period of 22–24 y and extreme spectral varia-

tions – from a typical Ap star to an extreme lanthanide star at rare earth element maximum. In the sense of extreme rotational spectral variations, then HD 96237 is comparable to HR 465, but has the tremendous advantage of a shorter 20.9-d rotation period, making its study in detail much more practical.

Figure 1 shows a triple line structure at the location of  $\lambda 6149 \text{ \AA}$  that is *not* caused by magnetic splitting. (The  $\lambda 6149 \text{ \AA}$  splitting would here have corresponded to a 6 kG field, which is inconsistent with other lines.) Comparison with the 2007 March spectrum (Fig. 2) shows that the blue-most component has disappeared while the two components centred around the  $\lambda 6149 \text{ \AA}$  line are replaced by a single, deeper, rather broad line. Our abundance estimates (Table 3) show a considerable increased iron abundance in the latest spectrum, while abundances of Nd and Pr have decreased on average more than 1.1 dex (Eu increased the same amount). The splitting of  $\lambda 6149 \text{ \AA}$  in the 2007 February spectrum is therefore most probably due to strong unidentified lines of, e.g., rare earths and a relatively low iron abundance. HD 101065 (Fig. 7 and 8) is a known case with precisely that condition. Abundances of Cr, Pr, Nd and Eu are greater than solar in both our HD 96237 spectra, while Fe is solar or near-solar. Ba  $\lambda 6141 \text{ \AA}$  is present in both spectra, and enhanced strongly in the most recent one.

HD 96237 does in fact have a  $\langle B \rangle \sim 3 \text{ kG}$  magnetic field which is responsible for the magnetic broadening of the iron  $\lambda 6149 \text{ \AA}$  line in Fig. 2. The high-resolution 2007 March spectrum reveals lines with partial Zeeman splitting and direct measurements of the splitting of  $\text{Cr I } 5116.049 \text{ \AA}$ ,  $\text{Cr II } 5220.912 \text{ \AA}$  and  $\text{Fe I } 6336.82 \text{ \AA}$  indicates a field of  $\langle B \rangle = 2.87 \pm 0.30 \text{ kG}$ , while a two-Gaussian fit to the  $\lambda 6149 \text{ \AA}$  line indicates  $\langle B \rangle < 3.27 \text{ kG}$ . A SYNTHMAG model with a 3.16 kG field ( $B_r = 3.0 \text{ kG}$  and  $B_m = 1.0 \text{ kG}$ ) is compared to these lines in Fig. 10. This quantity should be comparable to the mean magnetic field modulus, but in general not exactly equal to it as it is model dependent while  $\langle B \rangle$  is not. The same figure shows the 2007 February spectrum superposed the latest spectrum and although the Cr lines are not directly incompatible with the field strength, iron lines are useless in this spectrum due to this element's relatively low abundance. A single polarimetric measurement of HD 96237 was kindly obtained on 2008 January 23 (JD2454488.534) by Dmitri Kudryavtsev and Iosif Romanyuk using the Russian 6-m telescope at the SAO/RAS. (see Kudryavtsev et al. 2006 for a description of data reduction procedures and instrumentation.) It confirms the magnetic field with a longitudinal field of  $\langle B_z \rangle = -720 \pm 70 \text{ kG}$ . We are currently obtaining additional spectra of this important object.

3.3.14 *HD 110274*

Because of the small rotational broadening of HD 110274,  $v \sin i = 1 \text{ km s}^{-1}$ ,  $\lambda 6149 \text{ \AA}$  is magnetically resolved, in spite of a relatively weak field. After obtaining two spectra of the star with FEROS, we confirmed the discovery with a single UVES spectrum. The sharp-lined spectra have identical radial velocities for the FEROS spectra,  $\text{RV} = -6.04 \text{ km s}^{-1}$ , while 30 d later, the UVES spectrum appears slightly altered,  $\text{RV} = -6.59 \text{ km s}^{-1}$ . Considering that the wavelength calibrations were only checked with telluric lines, the common errors of the measurements overlap, and the star may



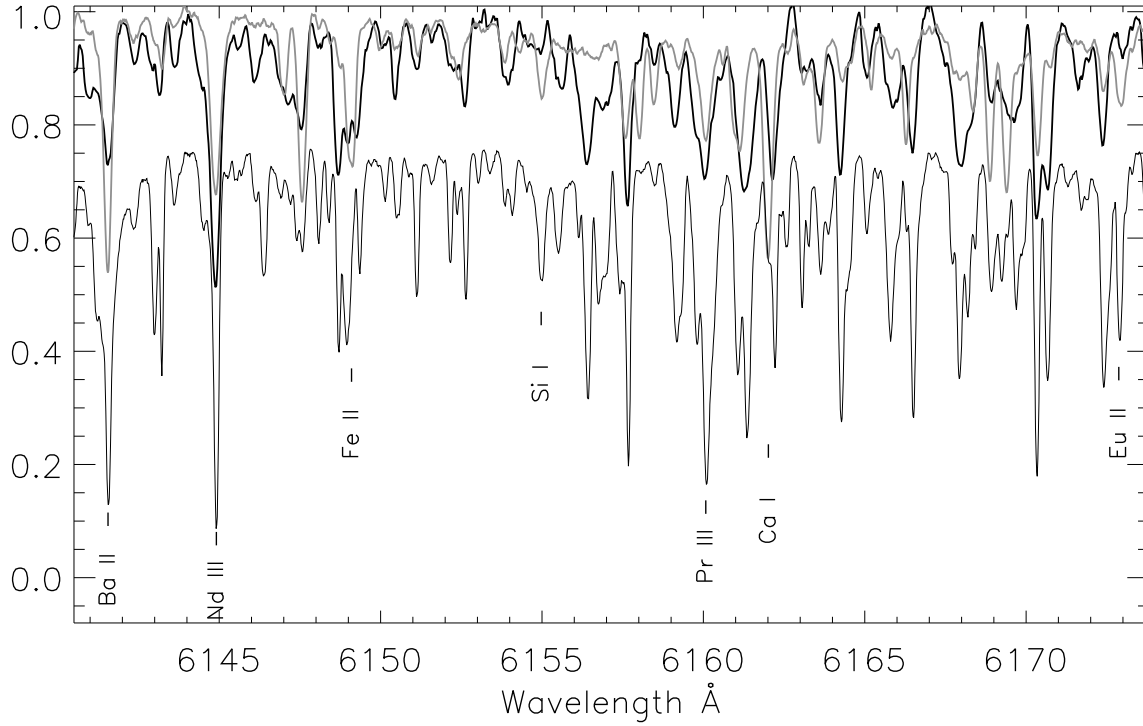


**Figure 8.** Same as Fig. 7, but for a region rich in elements such as Nd, Zr, Ce, Ba, La. The two HD 96237 spectra are from February (black thick line) and March (grey line). Note the extreme change from a highly peculiar spectrum to a typical Ap one, as well as disappearance and intensity changes in several lines.

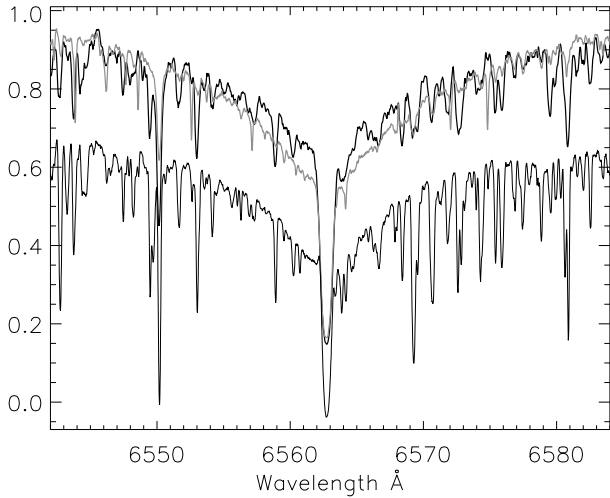


**Figure 7.** Spectral H $\alpha$  region for HD 96237 and the most peculiar known Ap star, HD 101065 (spectrum with thin line, shifted 0.25 downwards in intensity). The two upper HD 96237 spectra are from February (black thick line) and March (grey line). Ordinate is normalized intensity.

be radial velocity stable. With the  $\lambda 6149 \text{ \AA}$  line we measure a magnetic field strength of 3.80, 3.80 and 4.45 kG in chronological sequence ( $\langle B \rangle = 4.02 \pm 0.38 \text{ kG}$ , combined). This increase appears significant: with a total of 3 Fe, Cr lines (9 for the UVES spectrum, including Eu), we get correspondingly the measurements  $\langle B \rangle = 3.55 \pm 0.22$ ,  $3.73 \pm 0.57$  and

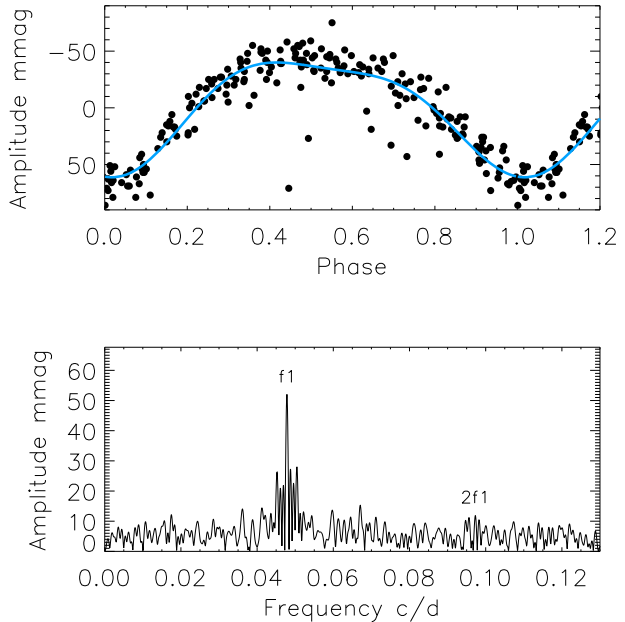


**Figure 9.** ASAS light curve of HD 96237 folded with the period of 20.9 d. Note the light curve's departures from a purely sinusoidal variation, which is reproduced well by including the first harmonic in the fit (superposed). Both frequencies are indicated in the amplitude spectrum in the bottom panel.

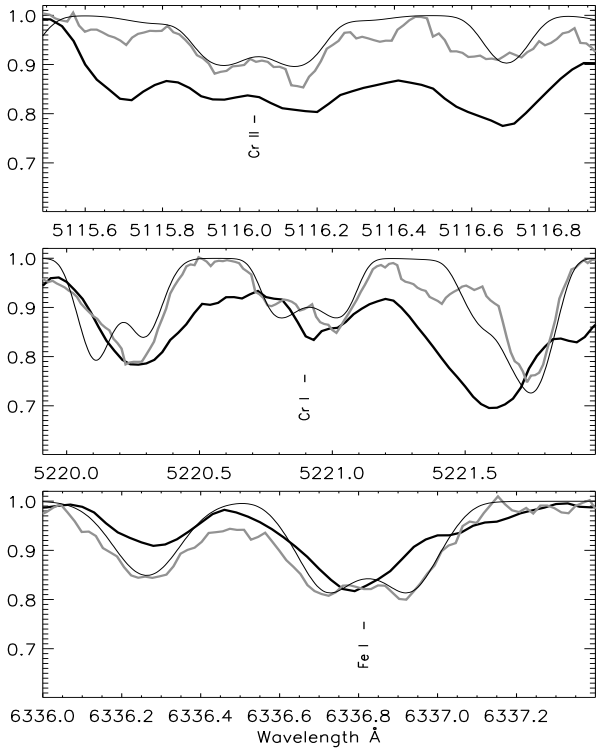


**Figure 10.** Magnetic field of HD 96237. The magnetically sensitive lines Cr I 5116.049 Å, Cr II 5220.912 Å and Fe I 6336.824 Å (top to bottom panels) of the 2007 February (thick black line), 2007 March (grey line) and a model spectrum superposed for a 3.2 kG field (3 kG radial and 1 kG meridional field). Landé factors of the three lines are  $g_{\text{eff}} = 2.92$  ( $\lambda$  5116.049), 3.00 ( $\lambda$  5220.912) and 2.00 ( $\lambda$  6336.824). Direct measurements of the splitting of the 2007 March spectrum gives the corresponding magnetic field strengths  $\langle B \rangle = 2.5, 2.8$  and 2.4 kG. The model is rotationally broadened to  $v \sin i = 4.5 \text{ km s}^{-1}$ . Ordinate is normalized intensity.

$4.55 \pm 0.50 \text{ kG}$ . The ASAS light curve shows a 265.3 d periodicity with 16 mmag amplitude ( $11.2 \sigma$ , Fig 11). *Hipparcos* photometry confirms this periodicity (249.5 d,  $5.0 \sigma$ ). The spectra show many continuum windows and lines of Ba, Ca and Si are present, though weak. Cr, Nd, Pr, Eu are greater than solar, Fe is near-solar.

### 3.3.15 HD 117290

For a clearly split  $\lambda 6149 \text{ \AA}$  line, we measure a constant magnetic field strength of 6.40, 6.38 and 6.36 kG, chronologically for three spectra ( $\langle B \rangle = 6.38 \pm 0.02 \text{ kG}$ , combined). The last measurement is separated by 30 d from the first two. Adding further 4–6 Fe, Cr, Eu, Nd and Ce lines to the analysis we get, within the errors, an unchanged field of  $6.27 \pm 0.82 \text{ kG}$  for all spectra combined. The radial velocity of HD 117290 is also constant ( $RV = -28.9 \pm 0.2 \text{ km s}^{-1}$ ) for the two spectra obtained on HJD 2454139 and 2454171.

The  $3\text{-}\sigma$  filtered ASAS photometry shows a 30 mmag decrease in brightness over 3.8 y (Fig. 12). The photometric scatter is considerable in the first half of the light curve and with no *Hipparcos* data for this star, more data for diaphragms smaller than those of ASAS are needed to confirm the trend. If this is associated with the stellar rotation, the shortest plausible period for a sinusoidal variation is 5.7 yr.

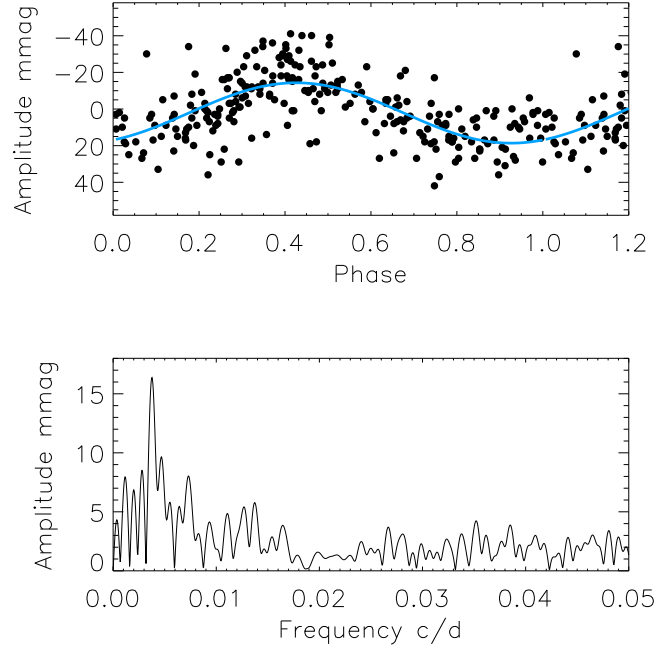


**Figure 11.** ASAS light curve of HD 110274 folded with the period of 265.3 d. Below is the corresponding amplitude spectrum.

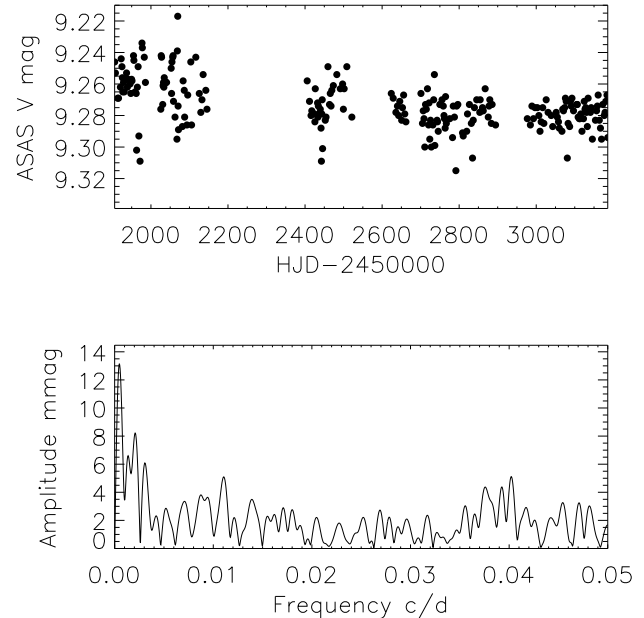


**Figure 12.** The 3.8 yr long ASAS light curve of HD 117290. A  $3\text{-}\sigma$  filter was applied to reject outliers from the light curve. Below is the corresponding amplitude spectrum.

Continuum windows are plentiful. Ba, Ca and Si are all over-abundant, as are Cr, Nd, Pr, Eu, while Fe is solar.

### 3.3.16 HD 121661

This star was observed twice, separated by 30 d. From  $\lambda 6149 \text{ \AA}$ , we measure in sequence a magnetic field strength of  $\langle B \rangle = 5.41$  and 6.92 kG (or  $6.16 \pm 1.07 \text{ kG}$ , combined). Compared to the small error,  $\sigma(\langle B \rangle) = 10 \text{ G}$ , for the weaker

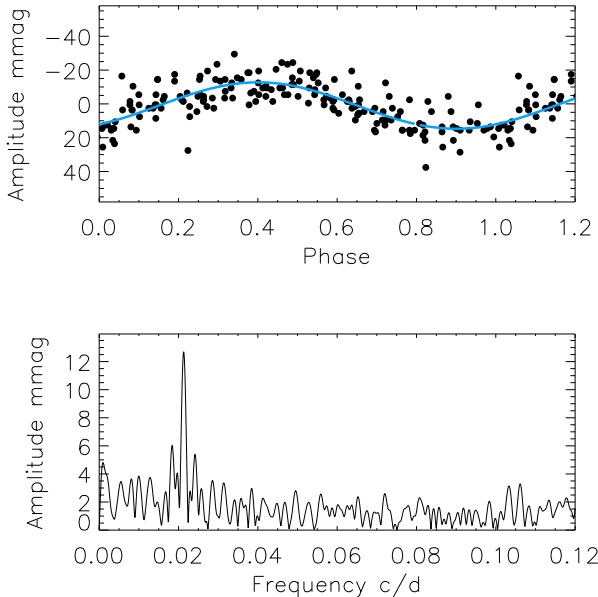


**Figure 13.** ASAS light curve of HD 121661 folded with a 47.0d period. Below: the corresponding amplitude spectrum.

magnetic field of HD 52847 measured from a relatively similarly shaped  $\lambda 6149 \text{ \AA}$  line and comparable span in time, the 1.51 kG change for HD 121661 is significant. From Figs. 1 and 2 one may also notice a considerable change in the Fe line’s shape. With 7 Fe and Cr lines (8 for the UVES spectrum, including Eu), we get  $\langle B \rangle = 5.40 \pm 0.47$  (2007 February) and  $\langle B \rangle = 6.01 \pm 0.82$  kG (2007 March). The radial velocity decreases marginally by about  $2\sigma$ :  $1.33 \pm 0.66 \text{ km s}^{-1}$  (from  $\text{RV} = 7.35 \text{ km s}^{-1}$  to  $\text{RV} = 6.02 \text{ km s}^{-1}$ , in sequence), but this needs to be confirmed before concluding the star is a radial velocity variable. The ASAS light curve in Fig. 13 shows a 47.0 d periodicity (14 mmag amplitude,  $13.7\sigma$ ) which is interpreted as the rotation period. Ba (including the  $\lambda 6141 \text{ \AA}$  line), Si I and Ca are absent or weak and many continuum regions are visible. Cr, Nd, Pr, Eu have greater than solar abundances while Fe is near-solar.

### 3.3.17 HD 135728AB

As a new SB2 binary star discovery, this star is of particular interest by having a magnetic component. The magnetic component has the next-to-weakest field in our FEROS study and was re-observed 32 d later with the high resolution of UVES. At that moment, the system was near orbital quadrature so the lines of the binary components are mostly merged, but the splitting of  $\lambda 6149 \text{ \AA}$  is evident in both spectra (Fig. 14). We measure in sequence the following radial velocities in the two spectra:  $-60.3 \pm 0.7$  and  $-17.2 \pm 0.4 \text{ km s}^{-1}$  for the primary, and  $+14.3 \pm 0.5$  and  $-32.7 \pm 0.1 \text{ km s}^{-1}$  for the secondary. With only two spectra, interpretation of dimensions of HD 135728 component’s is speculative. Nevertheless, to get a first impression of the system, we assume a circular orbit and not too different temperatures of the two stars. For this working hypothesis we here label the broader lined component (see Fig. 14)

the primary star, HD 135728A, as it appears to be more luminous and massive (see below), and the sharp-lined, magnetic component for the secondary star HD 135728B. The maximum observed radial velocity separation of the two stars,  $74.6 \text{ km s}^{-1}$ , indicates a relatively close orbit. The component spectra have exchanged relative locations in our two spectra, and the estimated systemic velocity is  $V_\gamma \sim -24.6 \text{ km s}^{-1}$ . The resulting observed RV amplitudes  $a_B$  and  $a_A$  thus constrain the orbital velocity amplitudes to  $K_A \geq 35.7 \text{ km s}^{-1}$  and  $K_B \geq 38.9 \text{ km s}^{-1}$ , leading to the mass ratio  $q = M_A/M_B = K_B/K_A \sim a_B/a_A = 1.09$ . The maximum period of the orbit can then be derived from:

$$M_A + M_B = \frac{(1 - e^2)^{3/2}}{2\pi G \sin^3 i} (K_A + K_B)^3 P. \quad (3)$$

By assuming: no eccentricity  $e = 0$ ; the sum of the radial velocity amplitudes  $K_A + K_B > 74.6 \text{ km s}^{-1}$ ; a mass of HD 135728A of  $M_A \sim 2.2 M_\odot$  (corresponding to the spectroscopic and photometric temperatures); and inclination  $i < 85 \text{ deg}$  (no eclipses are seen), then  $P < 96 \text{ d}$ . The true period can be an order of magnitude less, depending on the maximum radial velocity amplitudes.

At large separation, HD 135728B’s  $\lambda 6149 \text{ \AA}$  line indicates a field of  $\langle B \rangle = 3.89 \pm 0.11 \text{ kG}$ , and together with Cr I 5247.57  $\text{\AA}$  and Fe I 6336.82  $\text{\AA}$  a field of  $\langle B \rangle = 3.54 \pm 0.49 \text{ kG}$  is found. For the high-resolution 2007 March spectrum, the same 3 lines (here partly blended) provide  $\langle B \rangle = 3.43 \pm 0.52 \text{ kG}$ , or  $\langle B \rangle = 3.37 \pm 0.28 \text{ kG}$  for  $\lambda 6149 \text{ \AA}$  alone. This suggests a constant field strength of  $\langle B \rangle = 3.63 \pm 0.30 \text{ kG}$  based on the  $\lambda 6149 \text{ \AA}$  line. We cannot exclude a magnetic field of up to  $\sim 2.5 \text{ kG}$  for component A, which could be evaluated from a detailed analysis of magnetic broadening or moments of line profiles, such as described in Mathys & Hubrig (2006) and Freyhammer et al. (2008a).

The two component spectra are similar in the covered wavelength range (e.g. Si II 6347 and 6371  $\text{\AA}$ , Mg II 4481  $\text{\AA}$ , Ca II 8498  $\text{\AA}$ ), though with a different light ratio. The temperatures of the two stars therefore appear to be similar, Which, e.g., for the Ca II K region corresponds to an early-F type star. The photometric temperature for the combined light indicates a much higher temperature ( $T_{\text{eff}} = 8060 \text{ K}$ ). The ASAS V photometry shows no long-period variability above 6 mmag. We estimate from the double  $\text{H}\alpha$  line that HD 135728B only contributes to the total light with  $37 \pm 3$  per cent. This estimate was made by comparing a composite of two identical spectra, by applying only a wavelength shift and different light factors. Direct fitting of Gaussians to the blended  $\text{H}\alpha$  cores gives a similar light factor of the secondary star (35 per cent). The corresponding light ratio is  $\sim 1.70$ , which for the luminosity of the system in Table 2 leads to estimated individual luminosities of  $\log L_A \sim 1.40$  and  $\log L_B \sim 1.17 L_\odot$ , in reasonable agreement with the preliminary mass ratio.

Both components have greater than solar abundances of Cr, Nd, Pr and Eu, but considerably stronger rare earth elements in the secondary, magnetic, component (HD 135728B). Fe has near-solar abundance in the A component, and greater than solar abundance in the other star. We emphasise that the estimates in Table 3 are based on the much simplified assumption of same luminosities of the two stars. Ba  $\lambda 6141 \text{ \AA}$  is strong in both stars but considerably stronger in HD 135728A. HD 135728B has a weaker  $\text{H}\alpha$  line,

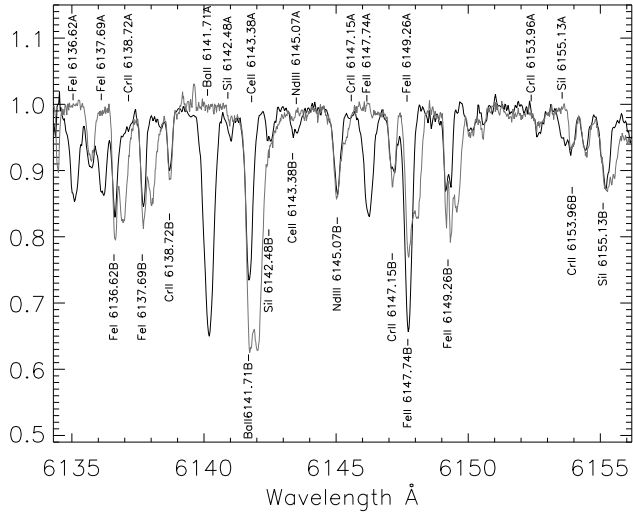


**Figure 14.** A region of our two spectra of the SB2 binary HD 135728AB, with the magnetic component shifted to rest wavelengths. Ordinate is normalized intensity. In the 2007 February spectrum (black), the primary star’s spectrum is shifted to shorter wavelengths than the secondary and to longer wavelengths in the 2007 March spectrum (grey). Locations of lines are indicated for both components in the 2007 February spectrum (black). Those referring to the broad-lined primary HD 135728A are indicated above the continuum (identifications ending on ‘A’), and below the continuum for the secondary HD 135728B (identifications ending on ‘B’). Note, e.g., the stronger Ba line of HD 135728A. Nd is strongest in HD 135728B and this star’s magnetically resolved Fe line at 6149 Å is obvious in both recorded spectra.

is more sharp lined ( $v \sin i = 2 \text{ km s}^{-1}$ ) and its  $\lambda 6149$  Å line is magnetically resolved. Ca is of similar strength in both stars, about  $-5.34$  dex. Also Sc is clearly present in HD 135728B, while only Sc II  $5657$  Å was identified in HD 135728A. The abundances of Sc also seem similar, which lends some support to HD 135728A being Ap. Neither of the stars have Nd or Pr ionization disequilibrium anomalies.

### 3.3.18 HD 143487

With a rather peculiar spectrum, this star is a particularly good roAp candidate. Comparing the 2007 February spectrum with the 2007 March (UVES) spectra, we find no change in the absolute radial velocity of the star ( $RV = -26.0 \text{ km s}^{-1}$ ). The Zeeman splitting of  $\lambda 6149$  Å indicates a constant magnetic field of  $\langle B \rangle = 4.23 \pm 0.07 \text{ kG}$  for all spectra. Including two more Cr lines, the composite UVES spectrum (Table 1) shows a field of  $\langle B \rangle = 4.30 \pm 0.16 \text{ kG}$ . No long-period variability above 6 mmag is detected in the photometry.

The spectrum of HD 143487 is highly peculiar and, e.g., Pr, Nd are among the strongest in this study. Also Cr and Eu abundances are greater than solar, while that of Fe is solar. Ba  $\lambda 6141$  Å is very shallow ( $< 5$  per cent below continuum). There is a clear ionization disequilibrium anomaly of Nd and Pr with  $\Delta[\text{Pr}]_{\text{III-II}} = 1.50$  and  $\Delta[\text{Nd}]_{\text{III-II}} = 1.36$ , in excellent agreement with empirical findings for roAp stars (Ryabchikova et al. 2004). With those anomalies and its relatively low temperature  $T_{\text{eff}} = 6930 \text{ K}$ , HD 143487 is a prime roAp star candidate.

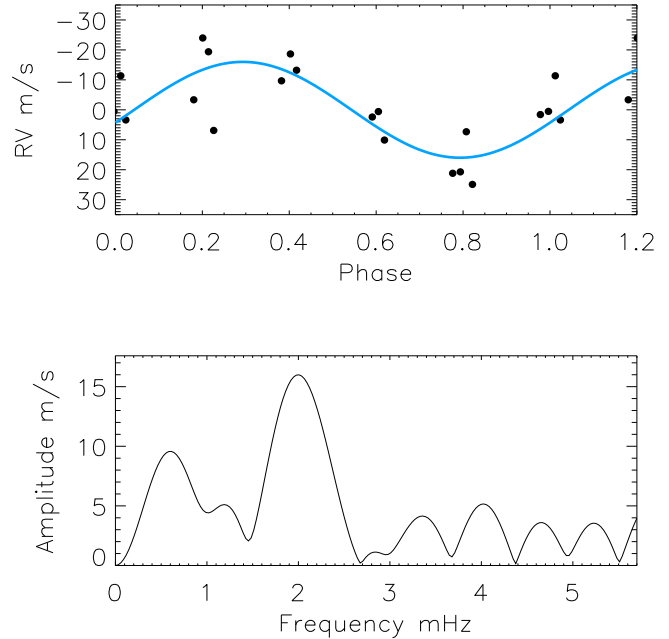


**Figure 15.** An initial probe for rapid pulsations in the radial velocities of 18 HD 143487 spectra. The top panel shows our 32 min radial velocity curve folded with a 2 mHz candidate period. The velocities are from cross-correlation of all spectra with an average spectrum. The bottom panel shows the corresponding amplitude spectrum. The data are de-trended for a linear drift. While the peak at 2 mHz is plausibly real, it needs confirmation.

We attempted detection of pulsations with UVES by obtaining 18 spectra in 32 min. Using the procedures described in Freyhammer et al. (2008a) the spectra were then searched for rapid pulsations, but due to the short run the results were inconclusive. An intriguing result, however, was that cross-correlation of the spectra with the average spectrum in the  $5150 - 5860$  Å region indicates (Fig. 15) a 2 mHz (8 minute) period at a  $4.6\text{-}\sigma$  level. This, however, could not be confirmed by detection of radial velocity variations in individual lines or groups of combined lines. Nevertheless, as the case of  $\beta$  CrB shows (Hatzes & Mkrtchian 2004; Kurtz et al. 2007), it is possible to detect roAp pulsation using large chunks of the spectrum when individual lines may not have sufficient  $S/N$  to show a clear signal. Fig. 15 makes a case for HD 143487 being a new roAp star, but we conservatively await confirmation of this. More data are now being collected for this purpose.

The spectral classification from the Michigan Catalogue with a note is *\*APEC. Overlapped; many lines; probably Sr, Eu, Cr, but many others also.*

## 4 DISCUSSION AND CONCLUSIONS

As part of a systematic search for new roAp candidates using FEROS on the ESO 2.2-m telescope, we have discovered 17 new magnetic stars with magnetically resolved lines and with these lines measured their mean magnetic field moduli directly. For 11 stars, spectra were obtained about 30 d later at higher resolution with UVES on the VLT. These were used to confirm the discoveries and check the stability of the measured magnetic field strengths and radial velocities.



A new double-lined spectroscopic binary, HD 135728AB, was discovered with two similar components, for one of which, the more slowly rotating component, a magnetic field was detected. It is possible that the primary (the faster rotating and more massive star, as deemed from its significantly smaller radial velocity difference between our two spectra) is either an Am or Ap star – i.e. either magnetic or non-magnetic; as yet we cannot tell. It is likely that the secondary is a spectrum variable (the primary may be also) so that the rotation periods of the stars can be determined independently and compared to the orbital period, thus showing whether either or both of the stars are synchronously rotating. Since both stars show overabundances typical of Ap and Am stars, a first guess might be that one is Am (non-magnetic) and the other Ap (magnetic). If that is so, how can two, rather similar stars in a close binary with both in the Ap-Am domain end up with one strongly magnetic and the other not? Or, on the other hand, if the primary *is* magnetic, but has a weaker field, then the question is similar, but not so extreme: how do the two components end up with different field strengths. There are Am-Am SB2 systems known – WW Aurigae is a famous eclipsing example where the stars are very similar in mass, but not identical in abundances. SB2 systems with a magnetic Ap star are very rare and HD 135728AB may be particularly promising for illuminating the magnetic field origin question. Examples of other such cases are: HD 59435 (Wade, Mathys, & North 1999), HD 55719 (Bonsack 1976) and HD 98088 (Abt et al. 1968; Hensberge 1974; Bychkov, Bychkova, & Madej 2005). These binaries have the following characteristics: magnetic periods of 5.8 – 1360 d, orbital periods of 5.9 – 1386.1 d, magnetic fields of 1.45 – 8 kG and companion-to-Ap star mass ratios of 0.75 – 1.33. In a recent study of the very young binary HD 72106, Folsom et al. (2007) established a dipole field of 1.3 kG for the primary star which rotates fast enough to permit these authors to produce 2-D surface abundance maps.

It is possible that two other systems in our sample are binary: HD 55540 had a significant radial velocity change, while HD 121661 needs confirmation of a marginally significant change. Neither of these systems, if confirmed, are of the importance of HD 135728AB and further observations are planned to determine the orbital period and use spectral disentanglement to study the abundances of both its components in detail.

The most important discovery, HD 75049, has the second-largest known magnetic field of any Ap star and was found to be highly variable in magnetic field strength and fine-structure over a time scale of 30 d. The extremely strong magnetic field may not only rival, but even surpass the strength of Babcock’s star (HD 215441), 34.4 kG. Follow-up is in progress of this very interesting object.

HD 96237 was shown to exhibit extreme abundance variations, possibly related to a photometric variability of 22 d that may be the rotation period. Extreme abundance variations with stellar rotation are known from more slowly rotating stars, such as HR 465 (HD 9996; Preston & Wolff 1970) for which Eu, Cr, Ca, Sr vary up to a factor of 3 in line strength (Cr and Eu in antiphase). A magnetic field was detected and measured. We compared the spectra of HD 96237 with those of the arguably most peculiar Ap star,

HD 101065, and demonstrated comparable levels of peculiar abundances. HD 96237 is remarkable by also exhibiting fast abundance variations. Follow-up studies are currently in progress of this important star.

From light curves in the ASAS database, the stars HD 75049, HD 88701, HD 96237, HD 110274, HD 121661, HD 117290 and HD 92499 were shown to be  $\alpha^2$  CVn variables. Two periods were detected for HD 75049, while HD 88701 exhibits a clear double wave. HD 117290 and HD 92499 show, as the only cases, variability longer than the time span covered by the photometry (3–5 years). There are some implications of the rotation periods found from the ASAS data and the measured rotational velocities, since these constrain the stellar radii and thus luminosities. An example we discussed is HD 88701 for which the rotation period and  $v \sin i$  implied an unexpectedly large radius. However, uncertainties in  $v \sin i$  measurements, sensitive to line-blending and magnetic broadening and the possibility of an ASAS period only being half of the rotation period (in case of double-wave light curves) leaves some uncertainties. Furthermore, astrometric luminosities suggest that at least half the stars are near the terminal end of the main-sequence, so that larger radii are to be expected in comparison with younger Ap stars.

Included among our original sample 140 cool Ap stars is HD 92499, a known magnetic star with Zeeman splitting (Hubrig & Nesvacil 2007). Our new spectra showed a constant magnetic field modulus and radial velocity of the star. As our target selection is relatively unbiased among more than 500 cool Ap stars, the fraction of such stars with magnetically resolved lines appears to be 13 per cent based on the first part of our Ap star survey.

Abundance estimates were used to identify Nd and Pr ionization disequilibrium anomalies in abundances of ions in the two first ionized states. HD 44226, HD 96237 and HD 143487 showed significant abundance anomalies ( $\sim 1$  dex) and are in addition to HD 92499 excellent rAp candidates. With 32 min time-series spectroscopy of HD 143487, we demonstrated a low-amplitude candidate period of 2 mHz that, however, could not be confirmed by individual lines.

We emphasise that the lack of accurate *Hipparcos* (ESA 1997) parallaxes [ $\sigma(\pi)/\pi < 0.2$ ] for the newly detected magnetic stars presented in this paper means that absolute magnitudes are considerably more difficult to determine because of the peculiar spectra of these stars. We note that for a subset of the stars having parallaxes, their relatively clustered location in the H-R diagram indicates that many of these are stars near the end of their main-sequence lifetimes. This new sample of stars with directly measured magnetic fields will aid studies of magnetic field interaction with stellar atmospheres. Polarimetric measurements are needed to establish geometry of the detected fields and to determine or confirm the rotation periods of the stars. We are currently obtaining high time resolution spectroscopy with UVES for 16 of the 18 stars in this study to search for rapid pulsations. The exceptions are HD 75049, which is too hot to be a rAp star, and HD 135728AB, which is an SB2 system.

**ACKNOWLEDGMENTS**

We thank the referee, Dr Stefano Bagnulo for a careful reading of the paper and many suggestions that helped to improve it. LMF, DWK and VGE acknowledge support for this work from the Particle Physics and Astronomy Research Council (PPARC) and from the Science and Technology Facilities Council (STFC). We are grateful for a magnetic measurement of HS 96237, obtained by by Dmitri Kudryavtsev and Iosif Romanyuk using the Russian 6-m telescope at the Special Astrophysical Observatory of the Russian Academy of Sciences (SAO/RAS). LMF received support from the Danish National Science Research Council's project 'Stellar structure and evolution - new challenges from ground and space observations', carried out at Aarhus University and Copenhagen University. We acknowledge extensive usage of the VALD, VizieR, SIMBAD, ADS (NASA) databases.

This paper has been typeset from a  $\text{\TeX}/\text{\LaTeX}$  file prepared by the author.

**REFERENCES**

- Abt H. A., Conti P. S., Deutsch A. J., Wallerstein G., 1968, *ApJ*, 153, 177
- Adelman S. J., 1973, *ApJS*, 26, 1
- Ashoka B. N., et al., 2000, *BASI*, 28, 251
- Asplund M., Grevesse N., Sauval A. J., 2005, *ASPC*, 336, 25
- Babcock H. W., 1958, *ApJS*, 3, 141
- Babcock H. W., 1960, *ApJ*, 132, 521
- Baliunas S. L., et al., 1995, *ApJ*, 438, 269
- Biémont E., Palmeri P., Quinet P., 1999, *Ap&SS*, 269, 635
- Bohlender, D. A., Landstreet, J. D., Thompson, I. B. 1993, *A&A*, 269, 355
- Bonsack W. K., 1976, *ApJ*, 209, 160
- Borra, E. F., Landstreet, J. D. 1979, *ApJ*, 228, 809
- Bruntt H., et al., 2008, *MNRAS*, 386, 2039
- Bychkov V. D., Bychkova L. V., Madej J., 2005, *A&A*, 430, 1143
- Castelli F., Kurucz, R. L., 2003, *IAUS*, 210, A20C
- Castelli F., Kurucz R. L., 2004, *astro*, arXiv:astro-ph/0405087
- Cowley, C. R., Ryabchikova, T., Kupka, F., Bord, D. J., Mathys, G., Bidelman, W. P. 2000, *MNRAS*, 317, 299
- Cowley C. R., Hubrig S., Ryabchikova T. A., Mathys G. et al. 2001, *A&A*, 367, 939
- Cowley C. R., Hubrig S., Kamp I., 2006, *ApJS*, 163, 393
- Cowley C. R., Hubrig S., 2008, *MNRAS*, 384, 1588
- Dorokhova T., Dorokhov N., 2005, *JApA*, 26, 223
- Elkin V. G., Riley J. D., Cunha M. S., Kurtz D. W., Mathys G. 2005, *MNRAS*, 358, 665
- ESA 1997, The *Hipparcos* and *Tycho* Catalogues. ESA SP-1200
- Folsom C. P., Wade G. A., Kochukhov O., Alecian E., Catala C., Bagnulo S., Landstreet J. D., Hanes D. A., 2007, arXiv, 712, arXiv:0712.0771
- Freyhammer L. M., Kurtz D. W., Mathys G., Elkin V. G., Riley J., 2008a, *MNRAS*, 385, 1402
- Freyhammer L. M., Elkin V. G., Kurtz D. W., 2008b, *MNRAS*, submitted
- Gomez A. E., Luri X., Grenier S., Figueras F., North P., Royer F., Torr Mennessier M. O., 1998, *A&A*, 336, 953
- González J. F., Hubrig S., Kurtz D. W., Elkin V., Savanov I., 2008, *MNRAS*, 114
- Griffin R. and Griffin R., 1973, *MNRAS*, 162, 255
- Handler G., Paunzen E., 1999, *A&AS*, 135, 57
- Hatzes, A. P., Mkrtichian, D. E. 2004, *MNRAS*, 351, 663
- Hensberge, H. Manfroid, J. Renson, P., Schneider, H. et al., *A&A*, 132, 291,
- Hensberge G., 1974, *A&A*, 32, 457
- Houk N., 1978, Ann Arbor : Dept. of Astronomy, University of Michigan : distributed by University Microfilms International, 1978, QB6.H,
- Houk N., 1982, Michigan Spectral Survey, Ann Arbor, Dep. Astron., Univ. Michigan, Vol. 3 (1982), 0
- Houk N., Cowley A. P., 1975, University of Michigan Catalogue of Two-Dimensional Spectral Types for the HD Stars, Univ. of Michigan, Vol. 1
- Houk N., Smith-Moore M., 1988, Michigan Spectral Survey, Ann Arbor, Dept. of Astronomy, Univ. Michigan Vol. 4
- Hubrig S., North P., Schöller M., Mathys G., 2006, *Astr.Nachr*, 327, 289
- Hubrig, S. and Nesvacil, N., 2007, *MNRAS* 378, L16
- Hubrig S., et al., 2005, *A&A*, 440, L37
- Jones, T. J., Wolff, S. C., Bonsack, W. K. 1974, *ApJ*, 190, 579
- Kochukhov O., 2006, *A&A*, 454, 321
- Kochukhov, O., Bagnulo, S., Barklem, P. S. 2002, *ApJ*, 578, L75
- Kudryavtsev D. O., Romanyuk I. I., Elkin V. G., Paunzen E., 2006, *MNRAS*, 372, 1804
- Kupka F., Piskunov N., Ryabchikova T. A. et al., 1999, *A&AS*, 138, 119 (<http://www.astro.uu.se/~vald/>)
- Kurtz D. W., Elkin V. G., Cunha M. S., Mathys G. et al. 2006, *MNRAS*, 372, 286
- Kurtz D. W., Elkin V. G., Mathys G., 2006, *MNRAS*, 370, 1274
- Kurtz D. W., Elkin V. G., Mathys G. 2007, *MNRAS*, 380, 741
- Landstreet J. D., Bagnulo S., Andretta V., Fossati L., Mason E., Silaj J., Wade G. A., 2007, *A&A*, 470, 685
- Lenz P., Breger M., 2005, *Communications of Asteroseismology*, 146, 53
- Linsky J. L., 1999, *ASPC*, 158, 3
- Luri X., Mennessier M. O., Torra J., Figueras F., 1996, *A&AS*, 117, 405
- Martinez P., 1993, Univ. of Cape Town, PhD thesis
- Martinez P., Kurtz D. W., 1994, *MNRAS*, 271, 129
- Mathys G. 1989, *FCPh*, 13, 143
- Mathys G. 1991, *A&AS* 89, 121
- Mathys G., Hubrig S., Landstreet J.D., Lanz T., Manfroid J., 1997, *A&AS*, 123, 353
- Mathys G., Hubrig S., 2006, *A&A*, 453, 699
- Michaud G., Charland Y., Megessier C., 1981, *A&A*, 103, 244
- Moon T.T., Dworetzky M.M., 1985, *MNRAS*, 217, 305
- Nelson M. J., Kreidl T. J. 1993, *AJ*, 105, 1903
- North P., Cramer N., 1984, *A&ASS*, 58, 387
- Piskunov N. E., 1992, *Stellar Magnetizm*, ed. Yu. V. Glagolevsky, & I. I. Romanjuk (St. Petersburg, Nauka), 92
- Piskunov, N. E., 1999, in 2nd International Workshop

- Kluwer Acad. Publ. ASSL, 243, 515
- Pojmanski, G., Acta Astronomica, 52, 397
- Preston G. W., Wolff S. C., 1970, Apj, 160, 1071
- Ryabchikova T., Piskunov N., Kochukhov O., Tsymbal V., Mittermayer P., Weiss W. W., 2002, A&A, 384, 545
- Ryabchikova T., Nesvacil N., Weiss W. W., Kochukhov O., Stütz C., 2004, A&A, 423, 705
- Ryabchikova T., Leone F., Kochukhov O., 2005, A&A, 438, 973
- Ryabchikova T., et al., 2006a, A&A, 445, L47
- Ryabchikova T., Ryabtsev A., Kochukhov O., Bagnulo S., 2006b, A&A, 456, 329
- Ryabchikova T., Mashonkina L., Ryabtsev A., Kildiyarova R., Khristoforova M., 2007, CoAst, 150, 83
- Samus N. N., Durlevich O. V., et al., 2004, Combined General Catalog of Variable Stars (GCVS4.2, 2004 Ed.), Institute of Astronomy of Russian Academy of Sciences and Sternberg State Astronomical Institute of the Moscow State University (2004), 2250, 0
- van Leeuwen F., 2007, A&A, 474, 653
- Wade G. A., Mathys G., North P., 1999, A&A, 347, 164
- Wade G. A., Ryabchikova T. A., Bagnulo S., Piskunov N., 2001, ASPC, 248, 373
- Weiss W. W., Ryabchikova T. A., Kupka F., Lueftinger T. R., Savanov I. S., Malanushenko V. P., 2000, ASPC, 203, 487
- Wolff S. C., Wolff R. J., 1971, AJ, 76, 422

APPENDIX A: ADDITIONAL FIGURES

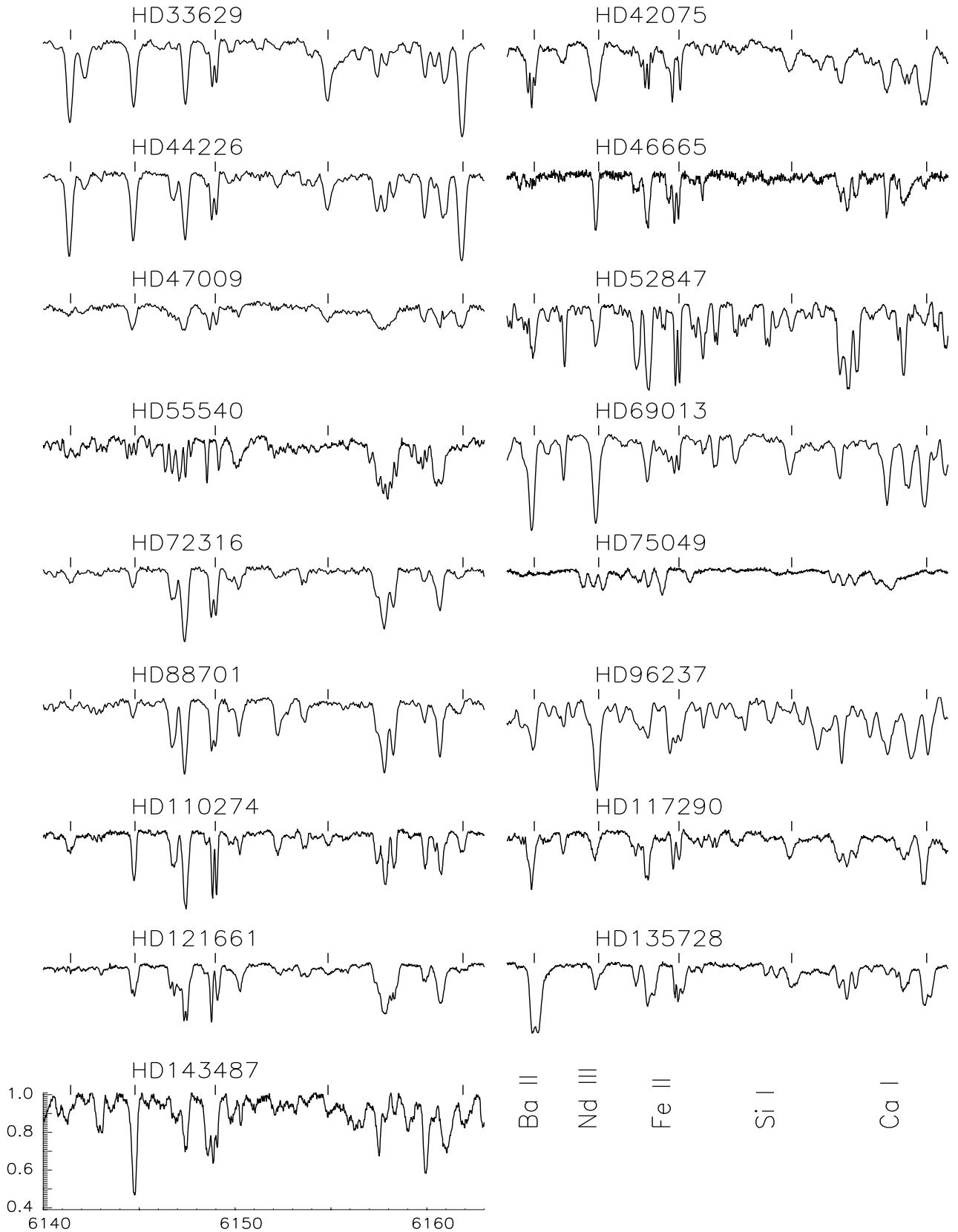


**Figure A1.** Line strengths for all the new magnetic stars, shown for the same selected region. All spectra are shifted to the laboratory wavelengths and plotted with same scale. Ordinate is normalized intensity. Locations of 5 different lines are indicated.



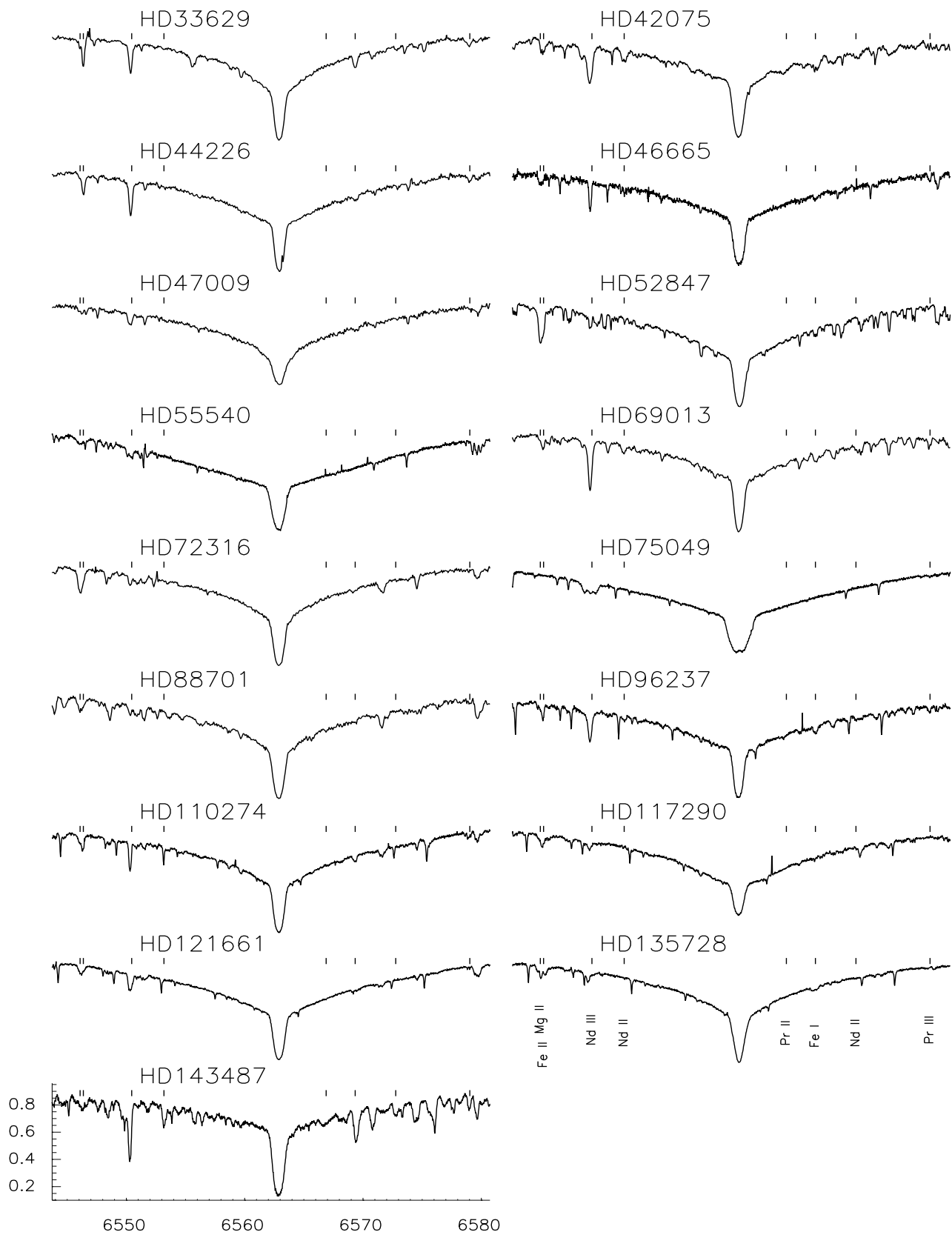


Figure A2. Same as Fig. A1, but for the inner H $\alpha$  region.